

Review of multiphoton absorption in crystalline solids

Vaidya Nathan and A. H. Guenther

Air Force Weapons Laboratory, Kirtland Air Force Base, New Mexico 87117

S. S. Mitra

University of Rhode Island, Kingston, Rhode Island 02881

Received June 4, 1984; accepted October 10, 1984

An extensive review of theoretical and experimental investigations conducted over the last two decades since the advent of the laser and relating to the simultaneous absorption of one or more photons by the valence electrons of a crystalline solid is given. The following topics are addressed, with greatest emphasis on the most recent results: the pioneering models of Braunstein and Ockman and that of Basov for two-photon absorption in direct-gap crystals, based on second-order time-dependent perturbation theory and parabolic and isotropic energy bands; extensions and modifications of the above models by various authors to take into account the effects of excitons, crystal anisotropy, laser polarization, and nonparabolicity as well as degeneracy of the electronic energy bands; rigorous band-structure calculations that employ realistic energy bands and momentum matrix elements that include many intermediate states to obtain good convergence in the perturbation calculation; the semiclassical theory of Keldysh that takes into account electric-field effects on the electronic energies and wave functions and that employs first-order perturbation theory to obtain multiphoton transitions of all orders; the fully quantized treatment of the multiphoton absorption (MPA) process along the above lines by Kovarskii and Perlin; the Volkov approximation method of Jones and Reiss; descriptions of the various experimental techniques that are usually employed to study nonlinear phenomena in solids; critical comparison between different theoretical predictions and experimental data; and finally, theoretical and experimental work relating to phonon-assisted two-photon transitions, three-photon absorption, four-photon absorption, and higher-order MPA processes in crystalline solids.

1. INTRODUCTION

A. Motivation

Multiphoton absorption (MPA) processes in crystalline solids have been the subject of extensive theoretical and experimental investigations since the advent of the laser over two decades ago. This interest in MPA has been stimulated by the importance of nonlinear absorption in high-power laser technology as well as by its role in many fundamental aspects of solid-state physics. Nonlinear absorption plays a crucial role in limiting the transparency of optical window materials and in causing laser-induced damage to optical components, particularly at short wavelengths. MPA processes have been successfully used to produce population inversion in semiconducting laser materials. This method has the advantage of producing a uniform concentration of electrons throughout the illuminated volume of the crystal rather than only over a skin depth, which is ordinarily obtained with linear absorption. MPA mechanisms have led to color-center production in alkali-halide crystals. Time-resolved spectroscopy after MPA affords information about the time scale and the physical processes involved in the creation of these color centers and excitons. Multiphoton absorbers can also be used as negative-feedback elements in laser cavities. They have been used for controlling laser pulse intensities and pulse durations. MPA techniques are extremely useful in studying the properties and processes associated with ultrashort laser pulses. This nonlinear spectroscopy has proved to be invaluable in determining the optical and electronic properties of crystalline solids; e.g., when one-photon absorption is for-

bidden by selection rules, a higher-order MPA may be allowed; under these conditions, MPA serves a unique purpose. Even in the case in which one-photon absorption is allowed, MPA experiments are still useful. In one-photon spectroscopy, most of the experimentally studied properties are characteristic of the surface rather than of the crystalline volume because of the drastic attenuation of the radiation as it propagates into the sample. MPA experiments, on the other hand, can enable one to study the properties truly characteristic of the crystalline volume because of the significantly smaller values of the MPA coefficients. MPA processes normally involve all the energy bands of the solid as intermediate states, and hence even a single MPA experiment, when used in conjunction with other relevant experimental or theoretical data, can give detailed information about the energy-band structures not readily attainable by using linear techniques. For these and numerous other reasons, the study of MPA processes in crystalline solids is extremely revealing and broad.

B. Scope

The subject of MPA has been pursued theoretically using both microscopic and macroscopic approaches. In the former, one calculates the MPA coefficients from the multiphoton-induced electronic transition probabilities. This is the general approach that is followed in this review. In the latter approach, the MPA coefficients are obtained from the imaginary parts of the higher-order nonlinear susceptibilities. The reader interested in this method is referred to the review articles by Bredikhin *et al.*¹ and Mahr.² We choose the $\mathbf{A} \cdot \mathbf{p}$ description for the interaction Hamiltonian and discuss only

the case of the simultaneous absorption of two or more photons from a single laser beam. For discussion of the $\mathbf{E} \cdot \mathbf{r}$ formalism as well as the case of two or more sources of radiation of different frequencies, the interested reader is again referred to the review articles by Bredikhin *et al.*,¹ Worlock,³ and Mahr.² These articles also contain discussions of coherence effects, selection rules, and detailed descriptions of experimental investigations that are not specifically addressed herein. We concentrate here on the more recent findings in this field and discuss earlier work only when needed for continuity of thought, particularly when they were not included in the suggested earlier reviews.

C. Phenomenological Description

The MPA can be described in a phenomenological manner by the generalized Beer-Lambert law:

$$\frac{dI}{dx} = -\sum_n \alpha_n I^n, \quad (1)$$

where α_n is the n -photon absorption coefficient [$(\text{length})^{2n-3}/(\text{power})^{n-1}$], I is the light flux (in watts per square meter), and x is the propagation direction. If for a given field strength and frequency the n th-order process dominates, the attenuation rate of the light flux is

$$\frac{dI}{dt} = -\frac{c}{\sqrt{\epsilon_\infty}} \alpha_n I^n, \quad (2)$$

where c is the speed of light in vacuum and ϵ_∞ is the high-frequency dielectric constant of the material. The relation between I and the peak electric-field amplitude E_0 (V m^{-1}) as well as the photon number density N_{ph} (m^{-3}) is given by

$$I = E_0^2 (\epsilon_\infty)^{1/2} / 2Z_0 = \frac{c}{\sqrt{\epsilon_\infty}} \hbar \omega N_{\text{ph}}, \quad (3)$$

where Z_0 is the vacuum impedance. Accordingly, the rate of photon absorption per unit volume is expressed as

$$\frac{dN_{\text{ph}}}{dt} = \frac{\alpha_n}{\hbar \omega} I^n = -n \frac{dN_e}{dt}, \quad (4)$$

where N_e is the density of conduction electrons created by the n -photon absorption process. In terms of the transition rate $W (= dN_e/dt)$, α_n is given by

$$\alpha_n = \frac{2n\hbar\omega(2Z_0)^n W(E_0^{2n})}{\epsilon_\infty^{n/2} E_0^{2n}}. \quad (5)$$

2. TWO-PHOTON ABSORPTION

A. Direct Transitions

First we discuss the salient features of some of the more well-known models of two-photon absorption (TPA) that exist in the literature. A critical comparison of the various models among themselves and with available experimental data is made in Subsections 2.A.3 and 2.A.5.

1. Second-Order Perturbation Theories

The general theory of MPA processes in atomic systems was laid down in the early days of quantum mechanics by Göppert-Mayer,⁴ who used n th-order time-dependent perturbation theory to obtain an expression for the probability of the simultaneous absorption of n photons by a single atomic

electron. When this rudimentary theory is applied to a crystalline solid, one obtains the following expression for the probability of a direct electronic transition from an initial valence band v to a final conduction band c , accompanied by the simultaneous absorption of n photons, each of frequency ω :

$$W_n = \frac{2\pi}{\hbar} \int \left| \sum_m \sum_l \dots \sum_j \sum_i \frac{\langle \Psi_c | H | \Psi_m \rangle \langle \Psi_m | H | \Psi_l \rangle}{[E_m - E_l - (n-1)\hbar\omega]} \right. \\ \left. \dots \frac{\langle \Psi_j | H | \Psi_i \rangle}{(E_j - E_i - 2\hbar\omega)} \frac{\langle \Psi_i | H | \Psi_v \rangle}{(E_i - E_v - \hbar\omega)} \right|^2 \\ \times \delta[E_c(\mathbf{k}) - E_v(\mathbf{k}) - n\hbar\omega] \frac{d^3\mathbf{k}}{(2\pi)^3}. \quad (6)$$

In Eq. (6), W_n is the n th-order transition probability rate per unit volume; Ψ_i, Ψ_j, \dots are the Bloch functions of the crystalline electrons in bands i, j, \dots , whose energies are E_i, E_j, \dots , etc. The delta function expresses energy-conservation requirements, and the summations extend over all possible intermediate states. The \mathbf{k} integration is over the entire first Brillouin zone, and H is the interaction Hamiltonian: $H = (e/mc)\mathbf{A} \cdot \mathbf{p}$, where \mathbf{A} is the vector potential associated with the incident radiation and \mathbf{p} is the momentum operator for the electron. The n -photon absorption coefficient α_n is related to the n -photon transition probability W_n by the simple expression

$$\alpha_n = 2W_n n\hbar\omega/I^n, \quad (7)$$

where I is the incident radiation intensity and the factor 2 accounts for electron-spin degeneracy. (In order to reduce the number of subscripts, hereafter we will use the notation α, β, γ , and δ for one-, two-, three-, and four-photon absorption coefficients, respectively.) For the case of TPA, Eqs. (6) and (7) reduce to

$$W_2 = \frac{2\pi}{\hbar} \int \left| \frac{\sum_i \langle \Psi_c | H | \Psi_i \rangle \langle \Psi_i | H | \Psi_v \rangle}{(E_i - E_v - \hbar\omega)} \right|^2 \\ \times \delta[E_c(\mathbf{k}) - E_v(\mathbf{k}) - 2\hbar\omega] \frac{d^3\mathbf{k}}{(2\pi)^3}, \quad (8)$$

$$\beta = 4W_2\hbar\omega/I^2. \quad (9)$$

Occasionally the nonlinear absorptions are described in terms of absorption cross sections. In the case of TPA, the nonlinear cross section σ_2 is related to W_2 by

$$\sigma_2 = W_2/N(I/\hbar\omega)^2, \quad (10)$$

where N is the density of active atoms. Thus, from Eqs. (9) and (10), we have

$$\beta = 4\sigma_2 N/\hbar\omega. \quad (11)$$

As can be seen from Eq. (6), the problem of MPA is conceptually simple; however, the calculation of reliable numerical values from the MPA transition probabilities is extremely difficult since it requires knowledge of the interaction Hamiltonian matrix elements among all the eigenstates of the crystal and summations over all the energy bands. Furthermore, it is also necessary to have information relative to all the energy eigenvalues as functions of the wave vector \mathbf{k} throughout the first Brillouin zone. Even in Eq. (8), where

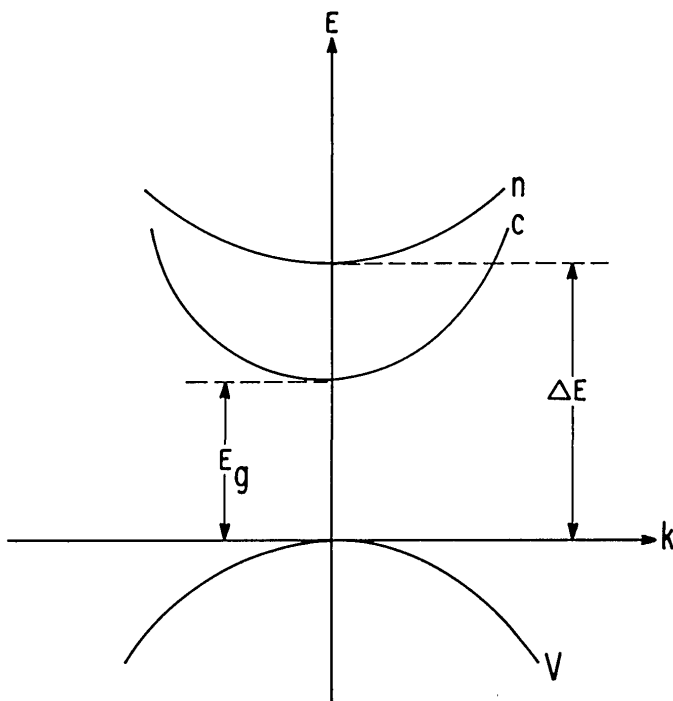


Fig. 1. Three-band model of Braunstein and Ockman⁵ for TPA in a direct-gap crystal.

there is only one summation, it extends over all possible intermediate states, and the above statements apply equally well.

In order to make the calculation of the absorption coefficients tractable, early workers usually made many approximations and simplifying assumptions regarding the energy bands, momentum matrix elements, and intermediate states, which considerably reduced the complexity of Eq. (6). However, as will be seen below, many of these approximations were not fully justified, and the calculated values of the MPA coefficients were thus suspect. Depending on the specific approximations made, the results of different calculations may vary significantly from one another. As an illustrative example, we will discuss, at some length, two well-known models employing different simplifying assumptions in an attempt to improve the calculational facility of Eq. (8). We will also briefly discuss many extensions and modifications of these two basic models. At the conclusion of this discussion, we will propose a more rigorous method of reliably evaluating W_2 from Eq. (8).

Braunstein and Ockman⁵ were the first to make an important simplification of Eq. (8) through the use of a three-band model (Fig. 1). The normal summation over intermediate states was replaced by a single higher conduction band. All three energy bands were assumed to be isotropic and quadratic functions of the wave vector \mathbf{k} . The interaction Hamiltonian was assumed to be of the form

$$H = \frac{e}{mc} \mathbf{A} \cdot \mathbf{p},$$

where \mathbf{A} is the vector potential associated with the incident radiation and \mathbf{p} is the momentum operator for the electron. The term proportional to \mathbf{A}^2 in the interaction Hamiltonian was neglected since its contribution to the transition probability was presumed negligibly small. Depending on the symmetries of the energy bands, either of the transitions from

the initial valence band (v) to the intermediate state (n) and from this intermediate state (n) to the final conduction band state (c) was dipole allowed or forbidden. Hence, three types of two-photon transition were possible: allowed–allowed (a-a), allowed–forbidden (a-f), and forbidden–forbidden (f-f). For allowed transitions, the interband momentum matrix elements were taken to be proportional to the interband energy difference, whereas, for forbidden transitions, they were proportional to the wave vector of the electron:

$$|\mathbf{P}_{ij}|_a^2 = \frac{m\hbar\omega_{ij}f_{ij}}{2}, \quad (12)$$

$$|\mathbf{p}_{ij}|_f^2 = \left(\frac{m}{m^+}\right)^2 (\mathbf{e} \cdot \mathbf{k})^2 \hbar^2, \quad (13)$$

where f_{ij} 's are the dimensionless oscillator strengths, m^+ is an effective mass for the transition, and \mathbf{e} is a unit vector for the photon polarization. The original formula as presented in the Braunstein paper contained a multiplicative error of ϵ_∞^{-2} (see Refs. 6 and 7). After making the correction, one obtains the following expressions for the TPA coefficients for a-a and a-f transitions:

$$\beta_{a-a} = \frac{2^{5/2}\pi e^4 (m_{vc}^*)^{3/2} \Delta E (\Delta E - E_g) f_{vn} f_{nc} (2\hbar\omega - E_g)^{1/2}}{3\epsilon_\infty c^2 m^2 (\hbar\omega)^3 \left[\Delta E - \hbar\omega + \frac{m_{vc}^*}{m_{vn}^*} (2\hbar\omega - E_g) \right]^2}, \quad (14)$$

$$\beta_{a-f} = \frac{2^{9/2}\pi e^4 (m_{vc}^*)^{5/2} \Delta E f_{vn} (2\hbar\omega - E_g)^{3/2}}{3\epsilon_\infty c^2 m (m^+)^2 (\hbar\omega)^3 \left[\Delta E - \hbar\omega + \frac{m_{vc}^*}{m_{vn}^*} (2\hbar\omega - E_g) \right]^2}. \quad (15)$$

In Eqs. (14) and (15), ϵ_∞ is the optical dielectric constant of the crystalline solid, m_{ij}^* 's are the reduced effective masses of bands i and j , ΔE is the minimum energy separation between bands v and n , and E_g is the energy gap between bands v and c (see Fig. 1).

Since the f-f transitions are much weaker than the other two cases, we omit the final formula for this case and note only that its dominant frequency dependence is of the form $\beta_{f-f} \sim (2\hbar\omega - E_g)^{5/2}$. It has been discussed in further detail by Braunstein and Ockman.⁵

Basov *et al.*^{8,9} proposed a simplification of Eq. (8) by using a two-band model, in which the initial and final bands themselves served as the intermediate states. They assumed the following Hamiltonian matrix elements for the intraband transitions:

$$H_{cc} = \frac{eA}{mc} \hbar k, \quad (16)$$

$$H_{vv} = \frac{eA}{m_v c} \hbar k, \quad (17)$$

and their final expression for β , after including the correction factor of 1/48 (Refs. 6 and 10), takes the form

$$\beta = \frac{2^{7/2}\pi e^4 E_g (2\hbar\omega - E_g)^{3/2}}{3\epsilon_\infty c^2 (\hbar\omega)^5 (m_{cv}^*)^{1/2}}. \quad (18)$$

In another vein, Loudon¹¹ extended the Braunstein model to take into account excitonic effects in a three-band model, in which the intermediate state was a higher conduction band

while the final state was an *s* exciton. His final result is quite similar to Braunstein's but multiplied by an excitonic envelope function that is frequently encountered in the theory of one-photon absorption. These excitonic effects, although important near the band edge, are negligible away from the band edge. Mahan^{12,13} also treated excitonic effects but in a two-band model, in which exciton levels were used for both intermediate and final states. The final electronic state was *s*, *p*, or *d* excitonic, depending on the symmetries of the valence and conduction bands. Bobrysheva *et al.*¹⁴ considered intermediate states in all excitonic levels in addition to those in the valence and conduction bands. Their calculations showed that, in CdS and Cu₂O, the contribution of the exciton states to the transition amplitude was 2 orders of magnitude smaller than that of the band state.

Bespakov *et al.*¹⁵ carried out model calculations including both interband and intraband transitions, anisotropy of the crystal, and the polarization of the radiation. Their final result had the form

$$\beta \sim k_1(2\hbar\omega - E_g)^{1/2} + k_2(2\hbar\omega - E_g)^{3/2}, \quad (19)$$

where k_1 and k_2 are coefficients whose magnitudes are such that, in general, the contribution of the second term was much smaller than that of the first term. Only in special cases in which the first term was very small was the second term significant. Hassan¹⁶ and Bassani and Hassan¹⁷ carried out a critical-point analysis of TPA in semiconductors. They concluded that sharp peaks in the frequency dependence of the TPA should occur, in correspondence to the saddle points in the electronic density of states. Their analyses showed that, whereas the TPA results were analogous to those for the one-photon process, the peaks and singularities were sharper, their intensities depending on the intermediate states. Hassan¹⁶ further obtained an expression for the TPA coefficients in anisotropic crystals by means of a three-band model similar to Braunstein's. In his analysis, energy bands were taken to be of the form

$$E_i(k) \sim \alpha_i(k_x^2 + k_y^2) + \beta_i k_z^2, \quad (20)$$

where α_i and β_i are the inverse effective masses of band *i* along the appropriate directions. Hassan's final formula for the TPA coefficient was similar to Braunstein's, and the two results coincided in the case of isotropic crystals when $2\hbar\omega \simeq E_g$.

Danishevskii *et al.*¹⁸ and Ivchenko¹⁹ showed that even in cubic crystals the TPA coefficient could depend on the laser polarization. They derived an expression for the ratio of the TPA coefficients for linear and circular polarizations in a narrow-gap semiconductor as a function of the laser frequency, using a model that consisted of two nonparabolic bands. Arifzhanov and Ivchenko²⁰ noted that in a three-band model the a-a TPA had a strong polarization dependence, whereas the a-f transitions had a weak dependence.

Fossum and Chang²¹ obtained a detailed expression for the TPA rate in InSb by employing the wave function previously derived by Kane²² on the basis of the $\mathbf{k} \cdot \mathbf{p}$ approximation. They also employed the second quantization formalism and included the statistics of the crystal electrons in the general expression for the TPA. Their final expression for the TPA rate had a frequency dependence of the form $(2\hbar\omega - E_g)^{3/2}$, similar to that of Basov,^{8,9} although the two formulas differed in the coefficients. Lee and Fan²³ made a major extension to

the Basov model by including the effects of excitons and valence-band degeneracies (Fig. 2). Using Kane's wave function, they considered intervalence-band transitions as well as the effects of a higher conduction band. They found that the contribution of the valence-band degeneracies and excitons to the TPA was significant, whereas that of the higher conduction band was small. Recently Pidgeon *et al.*²⁴ used a model that included the lowest conduction band, heavy-hole (hh), light-hole (lh), and spin-orbit-split bands, to calculate the TPA coefficients in zinc-blende-type semiconductors. The energy gaps separating the conduction band from the hh and lh bands were assumed to have the following nonparabolic dependence on the wave vector after Kane²²:

$$E_{c,hh}(\mathbf{k}) = \frac{E_g}{2} \left(1 + \frac{k^2 p^2}{3E_g^2}\right)^{1/2}, \quad (21)$$

$$E_{c,lh}(\mathbf{k}) = E_g \left(1 + \frac{8k^2 p^2}{3E_g^2}\right)^{1/2}. \quad (22)$$

In Eqs. (21) and (22), E_g is the energy separation between the conduction and degenerate valence bands at the Brillouin zone center and p is the momentum matrix element between the same bands. Their result showed that the frequency dependence of the TPA coefficients of zinc-blende-type semiconductors, when scaled by a factor $(1/E_g^3\epsilon_\infty)$, can be described by a universal curve (Fig. 3). They also concluded

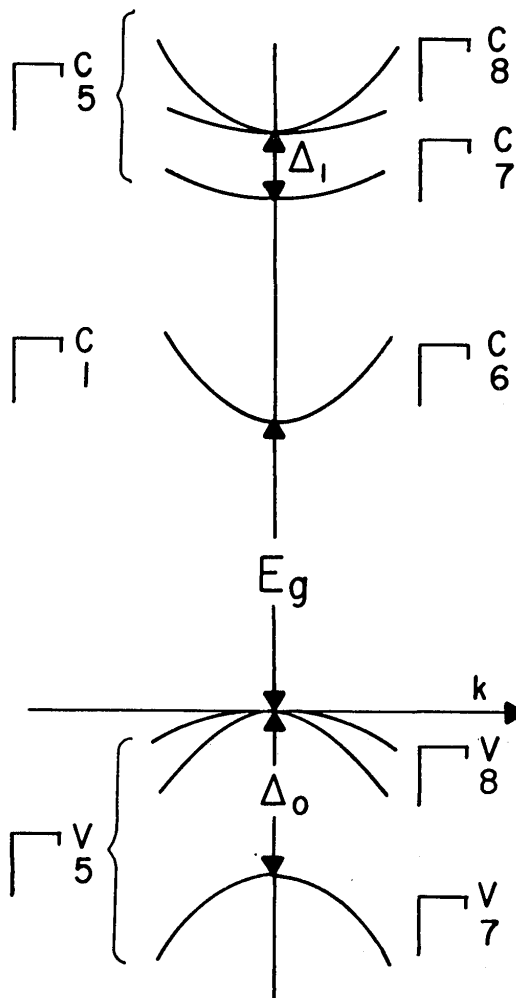


Fig. 2. Kane model²² for the energy-band structure of zinc-blende-type crystals. Δ_0 and Δ_1 are the spin-orbit splittings of the valence and higher conduction bands, respectively.

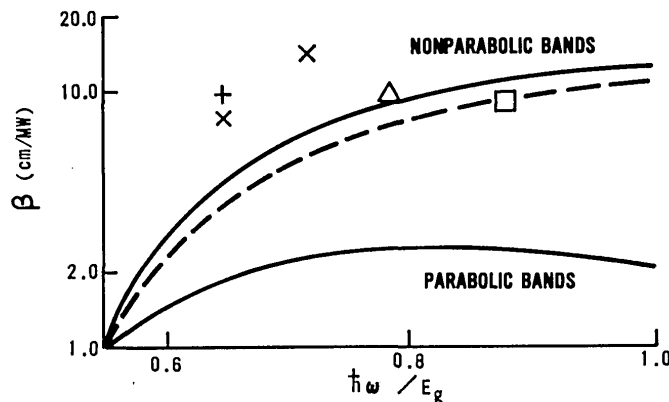


Fig. 3. Universal curve for the frequency dependence of β of zinc-blende-type semiconductors (after Pidgeon *et al.*²⁴). The various symbols denote the following crystals: +, Hg_{0.78}Cd_{0.22}Te; X, InSb; Δ, CdTe; and □, GaAs.

that when the two-photon energy was significantly larger than the energy gap, the parabolic model was seriously in error.

Vaidyanathan *et al.*²⁵ showed that the accuracy of the Braunstein result could be significantly improved if one used the intermediate state in the exciton levels instead of those in the higher conduction bands. Furthermore, they used the following nonparabolic expression for the wave-vector dependence of the conduction-band-valence-band energy difference (after Kane²²) in the Braunstein and Basov formulas:

$$E_{vc}(\mathbf{k}) = E_g \left(1 + \frac{\hbar^2 k^2}{\mu^* E_g} \right)^{1/2}. \quad (23)$$

In Equation (23), μ^* is the reduced effective mass of the two bands whose energy separation at wave vector \mathbf{k} is E_{vc} , for which E_g is the minimum direct energy gap. The effect of the nonparabolicity in this model was found to increase the TPA coefficients by a factor of about 2. Vaidyanathan *et al.*²⁶ also showed that in zinc-blende-structure semiconductors the predictions of the Basov formula approached the experimental data more closely if one included the degeneracy of the higher conduction band and considered the transitions as starting from the lh and split-off-hole bands in addition to those from the hh band. Recently, Bryant²⁷ calculated the TPA coefficient in Ge using the Kane model of the energy bands in which the matrix elements were evaluated using $\mathbf{k} \cdot \mathbf{p}$ theory and all bands within 10 eV of the valence-band edge were considered. Bryant found that for Ge it is essential that the spin-orbit split-off band be included as an intermediate state and the nonparabolicity of the conduction band be treated correctly.

More recently, Vaidyanathan *et al.*²⁸ carried out detailed band-structure calculations of the TPA coefficients of GaAs, InP, CdTe, and ZnSe within the context of second-order perturbation theory. They calculated the electronic energy bands and oscillator strengths throughout the first Brillouin zone by means of the empirical pseudopotential method (EPM) and evaluated the TPA coefficients by numerically integrating Eq. (8) (see Fig. 4). These authors considered transitions originating from the highest three valence bands (each band doubly degenerate because of spin) and ending in the lowest conduction band, whenever these transitions were energetically possible, and included the intermediate states in the highest four valence bands and the lowest thirty-one

conduction bands. The TPA coefficients obtained by them had a convergence of better than 0.01%. (When one more intermediate band was added, the resulting relative change in the TPA coefficient was less than 0.01%.)

Thus we see that there has been a steady improvement in the theoretical understanding of the TPA coefficients of crystalline solids based on second-order perturbation theory, starting with Braunstein in 1962 and continuing to date. We now turn our attention to models based on an entirely different approach to the problem of MPA in crystalline solids, i.e., the Keldysh approach. Comparison of the different theoretical models among themselves is deferred until Subsection 2.A.3, and comparison with the experimental data until Subsection 2.A.5.

2. Keldysh and Other Multiphoton-Absorption Theories of Arbitrary Order

Keldysh³⁰ viewed MPA as one limiting case of a more-general electric-field-induced effect that reduced to the well-known tunneling effect in the opposite limit. He assumed that the wave functions of the crystalline electrons in the presence of the radiation were described not by the usual Bloch functions but by modified Houston functions,³¹ which are approximate solutions of Schrödinger's equation for crystalline electrons in an electric field:

$$\Psi_{\mathbf{p}}^{c,v}(\mathbf{r}, t) = U_{\mathbf{p}(t)}^{c,v}(\mathbf{r}) \exp \left\{ \frac{i}{\hbar} \left[\mathbf{p}(t) \cdot \mathbf{r} - \int_0^t \epsilon_{c,v}[\mathbf{p}(\tau)] d\tau \right] \right\}, \quad (24)$$

where the time-dependent momentum

$$\mathbf{p}(t) = \mathbf{p} + \frac{e\mathbf{E}}{\omega} \sin \omega t \quad (25)$$

contains explicit information on the accelerated motion of the charges in both the conduction (*c*) and valence (*v*) bands under the action of the impressed electric field $\mathbf{E} = \mathbf{E}_0 \cos \omega t$. As a result of thus including a part of the electron-radiation interaction in the zeroth-order Hamiltonian, Kel-

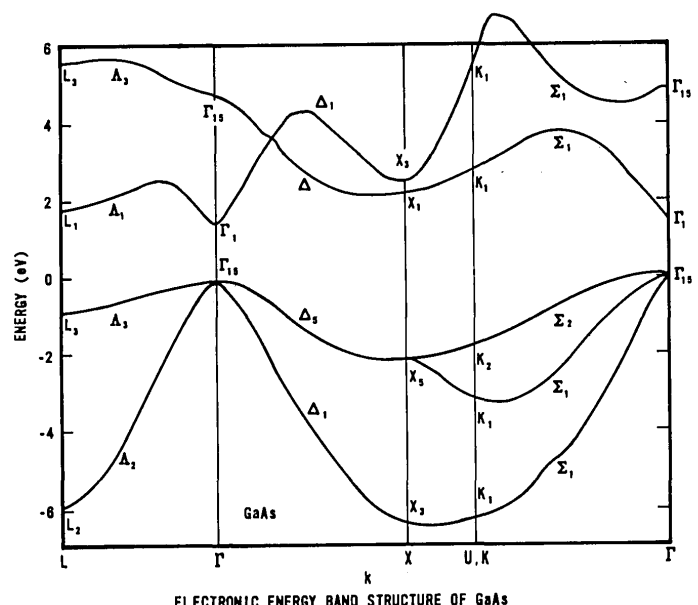


Fig. 4. Empirical pseudopotential band structure of GaAs (after Cohen and Bergstresser²⁹).

dysh was able to derive an expression for multiphoton transitions of all orders by employing just first-order perturbation theory. The following simple interpretation of the physics involved in the Keldysh theory is due in large measure to Weiler *et al.*³²: In the Keldysh model the electronic energy oscillates in time with the periodicity of the incident radiation. As a result, the electron is able to absorb not only at the fundamental frequency of the radiation but also at all higher harmonics.

Keldysh assumed that the electronic energy bands were nonparabolic, of the form generally described by Eq. (23). In the limiting case when the adiabaticity parameter given by

$$\gamma = \frac{\omega}{eE_0} (2\mu^* E_g)^{1/2} \quad (26)$$

(E_0 is the electric-field amplitude of the radiation) was much larger than unity, Keldysh obtained the following expression for the multiphoton transition rate per unit volume:

$$W = \frac{2\omega}{9\pi} \left(\frac{\mu^*\omega}{\hbar} \right)^{2/3} \left(\frac{e^2 E_0^2}{16\mu^* \omega^2 E_g} \right)^{\langle E_g/\hbar\omega + 1 \rangle} \times \exp \left[2(\tilde{E}_g/\hbar\omega + 1) \left(\frac{1 - e^2 E_0^2}{4\mu^* \omega^2 E_g} \right) \right] \times \Phi[(2\langle \tilde{E}_g/\hbar\omega + 1 \rangle - 2\tilde{E}_g/\hbar\omega)^{1/2}]. \quad (27)$$

In Eq. (27), the number of photons absorbed simultaneously is given by $\langle \tilde{E}_g/\hbar\omega + 1 \rangle$, where the notation $\langle \rangle$ means the integer part of the argument and \tilde{E}_g is the effective band-gap in the presence of the radiation:

$$\tilde{E}_g = E_g \left(1 + \frac{1}{2\gamma^2} \right). \quad (28)$$

In the opposite limit of $\gamma \ll 1$ corresponding to quantum-mechanical tunneling, the effective band-gap is given by

$$\tilde{E}_g = \frac{2}{\pi} E_g \frac{(1 + \gamma^2)^{1/2}}{\gamma} E \left[\frac{1}{(1 + \gamma^2)^{1/2}} \right], \quad (29)$$

where E is the complete elliptic integral of the second kind. The increase in the effective energy gap of the crystal is due to the intraband motion of the electrons superposed upon the interband transition. The function ϕ occurring in Eq. (27) is the Dawson integral given by

$$\phi(z) = \exp(-z^2) \int_0^z \exp(y^2) dy. \quad (30)$$

Since Keldysh, many workers have studied TPA in the presence of electric and magnetic fields using methods similar to that of Keldysh (see, for example, Yacoby,³³ Weiler *et al.*,³² Bychkov and Dykhne,³⁴ Kovarskii and Perlin,³⁵ and Jones and Reiss³⁶). Many of these authors have stated that the Keldysh formula is inaccurate or invalid when the order of the multiphoton process is small or when it is even. However, not enough proof has been advanced to support either of these claims generally. We discuss this point in Subsection 2.A.3, where we make a critical comparison between the Keldysh formula and second-order perturbation formulas.

We conclude this section by briefly discussing two more works relating to MPA processes, which proceed along lines similar to Keldysh's. Kovarskii and Perlin³⁵ considered the multiphoton transitions as arising from both the diagonal and the nondiagonal terms of the electron-photon interaction. They employed the second quantization formalism and used a three-band model consisting of the lowest conduction band,

the highest valence band, and the spin-orbit split-off valence band. Their final formula for MPA had the following frequency dependences:

$$\alpha_n \sim (n\hbar\omega - E_g)^{1/2}, \quad n \text{ odd},$$

$$\alpha_n \sim (n\hbar\omega - E_g)^{3/2}, \quad n \text{ even}.$$

This is in contrast to the Keldysh formulas, which had a one-half power dependence for all n .

Jones and Reiss³⁶ investigated the excitation of a valence electron into the conduction band of a crystalline solid in the presence of a circular polarized electromagnetic field of arbitrary intensity by using the S matrix technique. They found that for high intensities the Stark shift in the energy of the conduction band increased rapidly, making higher-order processes more probable than lower-order processes. For example, a TPA process energetically allowed in a given solid for a given laser frequency at low intensities became energetically impossible when the laser intensity was sufficiently increased. With the other parameters fixed, a three-photon process was needed instead. Physically, two photons cannot supply enough energy to oscillate the electron and still effect an interband transition; it would now take three photons to effect a multiphoton transition. This result is similar to that of Keldysh while differing markedly from the predictions of the conventional perturbation theories. On the other hand, their low-intensity result was identical with the perturbation result for all orders. Jones and Reiss's calculation also showed that for high enough intensities the transition rate became nearly independent of the number of photons simultaneously absorbed.

3. Comparison of Different Theoretical Models

Before making a comparison of the different theories with the experimental data, one can make the following comments regarding the merits and drawbacks of the different theoretical models. As was mentioned earlier, it has often been stated that the Keldysh formula is inaccurate or invalid when $\hbar\omega$ is a significant fraction of E_g as well as when the photon multiplicity is even. However, these statements have never been satisfactorily explained or proven. It has recently been shown that these notions are ill founded, and the Keldysh formula is at least as accurate as the conventional perturbation formulas, even in the case of one- and two-photon absorptions.^{10,25,26,37} In point of fact, it has been shown²⁶ that, close to the TPA edge, if one expands the Dawson integral encountered in the Keldysh formula in a series, the first term closely resembles Braunstein's formula for a-a transitions, while the second term relates with Basov's formula for a-f transitions within a numerical factor of ~ 3 . In the past it was also stated that the Basov formula predicted TPA coefficients that were significantly larger than the predictions of Keldysh and Braunstein. It has been shown that the above contention was actually the outcome of several apparent inaccuracies in the original Basov formula.^{6,25}

Among the formulas of Keldysh, Braunstein, and Basov, the one that is due to Braunstein is probably the least desirable to use for reliable predictions of the TPA coefficients since this formula needs information regarding the band parameters of a higher conduction band, which are frequently not accurately known from either theory or experiments. Depending on the approximations made with respect to the

higher conduction band, the results of the Braunstein formula could vary significantly in numerical prediction.

The formulas of Keldysh and Basov, although somewhat more reliable than Braunstein's, are still only approximate descriptions of the TPA process; their predictions are also suspect, especially away from the band edge, where some of the approximations regarding the energy bands and oscillator strengths may not be valid. To obtain more-reliable results, the following points should be considered. Close to the absorption edge, exciton effects should be included.²³ As one moves away from the band edge, the exciton effects become negligible, but the nonparabolicity of the bands becomes important.²⁴ Also, band degeneracies should be taken into account in these calculations.²⁶ For quantitative results of maximum reliability, one should use realistic energy bands and oscillator strengths throughout the Brillouin zone, obtained from band-structure calculations such as the EPM, the orthogonalized plane-wave method, the augmented plane-wave method, and the Korringa-Kohn-Rostoker method, and include all possible intermediate states. This was done by Vaidyanathan *et al.*, using EPM band structures for GaAs, InP, CdTe, and ZnSe.²⁸ Their results were dramatically different from those of earlier calculations, which used the simpler approximate expressions for the energy bands and oscillator strengths and inappropriately truncated the summation over the intermediate states.

The above remarks regarding the merits of different models were based solely on theoretical grounds. How well these models compare with the experiments is seen below after an examination is made of the experimental techniques and reported findings.

4. Experimental Techniques

Herein is a brief description of the general experimental techniques and methods of analysis used to deduce MPA coefficients. For information regarding the actual experimental arrangements and other details, the reader is directed to the original references.

The MPA coefficients are conventionally measured by means of one of the following three techniques: nonlinear transmission (NLT), nonlinear luminescence (NLL), or nonlinear photoconductivity (NLP) (Fig. 5). In NLT experiments, the radiation is allowed to pass through a sample

of the test material, whose dimensions are typically a few millimeters, and the transmitted intensity is measured as a function of the incident intensity. In the presence of both one- and two-photon absorptions, described by coefficients α and β , respectively, the change in the intensity of the light as it passes through the sample is given by [see Eq. (1)]

$$\frac{dI}{dx} = -\alpha I - \beta I^2, \quad (31)$$

when free carrier absorption is negligible.

The solution to the above equation is

$$T = \frac{I}{I_0} = \frac{(1-R)^2 \exp(-\alpha l)}{1 + \beta I_0(1-R)[1 - \exp(-\alpha l)]/\alpha}, \quad (32)$$

where R is the reflectivity at the wavelength of the incident radiation and l is the thickness of the sample. The reciprocal of the transmittance is usually plotted against the incident intensity to obtain a linear fit. The value of α is calculated from the intercept on the transmittance axis, and the value of β is deduced from the slope of the graph. The above analysis has been extended by Kleinman *et al.*³⁹ to the case of a Gaussian pulse with random fluctuations due to many longitudinal modes and by Danishevskii *et al.*⁴⁰ and by Gibson *et al.*⁴¹ to include the effects of free-carrier absorption. The most complete treatment of free carrier absorption (FCA) is that due to Gibson *et al.*⁴¹ These authors showed that the theoretical plot of $1/T$ as a function of the incident intensity was nearly a straight line, over most of the intensity range, even when the FCA was dominant over the TPA; hence the linearity of this graph cannot be taken as an evidence for the absence of the FCA. These authors estimated that in *n*-type InSb (6×10^{16} electrons/cm³), the FCA was about 100 times stronger than TPA for 200-nsec pulses of a CO₂ laser at an intensity of 1 MW/cm²; in *n*-type Ge, the relative strength of the two processes was nearly a factor of 10 for HF laser (2.6-3-μm-wavelength) pulses of duration 480 nsec and intensity 0.1 MW/cm². Their work shows the importance of properly including FCA in the analysis of the results of NLT and NLP in order to determine the TPA coefficient correctly.

In the NLP method, the total charge Q induced by multiphoton transitions is measured. In the case of TPA, Q is related to the TPA cross section σ_2 by

$$Q = eV_0NL\mu\tau^2[1 - \exp(-\tau_L/t)] \frac{\sigma_2 I_0^2}{1 + 2LN\sigma_2 I_0}, \quad (33)$$

where V_0 is the collecting voltage, L is the thickness of the sample, μ is the mobility of the conduction electrons, τ is their lifetime, N is the concentration of active atoms, and τ_L is the laser-pulse duration. By making certain assumptions about the values of the unknown parameters, σ_2 is deduced from the experimentally measured Q .

In NLL experiments, the density of conduction electrons produced by the multiphoton processes is inferred from the luminescent radiation produced as a result of the subsequent recombination of the generated electrons and holes. Often the luminescent intensity is plotted as a function of the incident flux of photons on a log-log graph, and the slope of this graph immediately gives the order of the multiphoton transition.

Each of the above three methods has its own merits and drawbacks. NLT and NLP are easily dominated by impurity effects, and it is often difficult to deduce the nonlinear cross section from NLL data because of the lack of knowledge of the

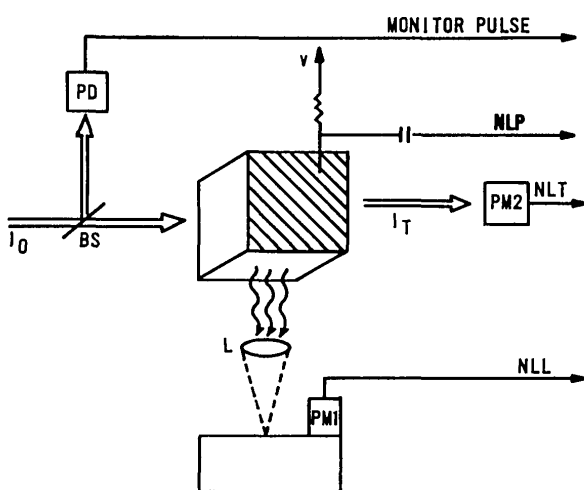


Fig. 5. Schematic of the experimental setup for the simultaneous measurements of NLT, NLP, and NLL in a crystalline solid (after Catalano *et al.*³⁸).

quantum efficiencies involved. Both NLP and NLL are complicated functions of carrier lifetime, mobility, etc., the values of which are seldom known reliably. As we have already seen, FCA can significantly affect experimental MPA coefficients. Furthermore, in NLT experiments the effects of self-induced transparency can be important, especially for ultrashort pulses and low temperatures. The self-induced transparency essentially consists of the resonance absorption and reemission of the radiation when the pulse duration is shorter than the transverse relaxation time of the electrons. This introduces a strong dependence of the measured nonlinear absorption coefficients on the laser-pulse duration and crystalline temperature (see Refs. 42 and 43). The effects of self-focusing, spatial and temporal fluctuations of the laser, and saturation of absorption that are due to filling of the energy bands can be important as well (see Refs. 44 and 45). There is the additional possibility that the increase in the effective band gap of the crystal at high radiation intensities can significantly alter the nature of the MPA processes.³⁶

All the aforementioned conventional methods suffer from their strong dependence on the parameters of the laser used, which unfortunately are often poorly characterized or are incompletely included in the analysis. In an attempt to overcome this shortcoming, a few different techniques for the measurement of the absolute and relative values of the MPA coefficients were recently reported in the literature. In the first method, the laser is well characterized, and the analysis of the data fully takes into account all the laser parameters.^{45,46} This method, however, restricts the range of frequencies in which the experiments can be done to those of the well-characterized lasers. The second technique is independent of the laser parameters and involves an absolute calibration of the TPA coefficients using other reliably known, nonlinear cross sections.⁴⁷ A disadvantage of this technique is the assumption that the quantum efficiencies of fluorescence at a given frequency and at its second harmonic are the same. Calibrations have also been done with respect to the well-known Raman-scattering cross sections. Lotem and Lynch⁴⁸ have proposed a two-channel normalization technique in which identical laser pulses are transmitted through the test sample and a reference sample, which permits determination of the relative TPA coefficients to an accuracy of $\pm 10\%$. Lotem and de Araujo⁴⁹ have reported a method for the direct measurement of TPA coefficients relative to known inverse Raman cross sections in which the dependence on the laser parameters was eliminated by the two-channel normalization method. Recently, Bass *et al.*⁵⁰ demonstrated the usefulness of laser calorimeters with sensitivity as high as one part in 10^5 to measure the TPA coefficients in crystalline solids.

5. Experimental Results and Comparison with Theory

As was already mentioned, we intend to discuss only the simultaneous absorption of several photons from a single laser beam. Furthermore, since the review articles by Worlock³ and Mahr² contain detailed discussions of most of the experimental data up to their times of publication, we will concentrate mostly on the more-recent experiments. Relevant experimental work dating before 1975 will be discussed only in those cases in which they were omitted in the above reviews.

Ashkinadze *et al.*⁵¹ measured the TPA coefficients of GaP

(direct energy gap ~ 2.8 eV, indirect energy gap ~ 2.2 eV) at $0.694 \mu\text{m}$ by NLP at 77 and 300 K. They used giant ruby pulses of duration 50 nsec and peak power 20 MW on three different samples of GaP of typical dimensions $5 \text{ mm} \times 2 \text{ mm} \times 0.22 \text{ mm}$ (an undoped crystal, a *p*-type crystal activated with Sm and with carrier density $\sim 10^{17}/\text{cm}^3$, and a *p*-type crystal activated with Gd and with carrier density $\sim 10^{18}/\text{cm}^3$). Only in the case of the third sample did they observe a strictly quadratic lux-ampere characteristic, typical of TPA. Using these data, they deduced a value of 0.1 cm^{-1} for the TPA coefficient at an intensity of 50 MW/cm^2 ($\beta = 4 \times 10^{-3} \text{ cm/MW}$).

Zubov *et al.*⁵² performed NLT measurements on single crystals of Ge with light from a *Q*-switched CaF₂:Dy²⁺ laser ($\lambda = 2.36 \mu\text{m}$) and obtained $\beta = 1 \text{ cm/MW}$ at room temperature [$E_g^d = 0.8 \text{ eV}, \hbar\omega (2.36 \mu\text{m}) = 0.525 \text{ eV}$].

Ralston and Chang^{53,54} measured the TPA coefficients of CdSe, CdTe, and GaAs at 300 K by the NLT technique with a *Q*-switched Nd:YAG laser. They found the TPA coefficients of CdSe and CdTe to be approximately 0.2 cm/MW , whereas that of GaAs was about 10 times smaller.

Danishevskii *et al.*¹⁸ experimentally studied the polarization dependence of TPA in InSb using CO₂ laser light for different values of the parameter $\hbar\omega/E_g$. This was achieved by using the 9.5- and 10.6- μm lines of the laser and also by varying the value of E_g by changing the sample temperature. The experimental values of the ratio $W_2^{\text{linear}}/W_2^{\text{circular}}$ for different values of $\hbar\omega/E_g$ agreed well with their theoretical prediction.

Catalano *et al.*⁵⁵ carried out NLP measurements on color-center-free single crystals of KI of dimensions $0.8 \text{ cm} \times 0.2 \text{ cm} \times 1 \text{ cm}$ at room temperature using the second harmonic of a ruby laser at a maximum power of 10 MW. They obtained a value of $(5 \pm 0.5) \times 10^{-49} \text{ cm}^4 \text{ sec}$ for the TPA cross section. From Eq. (11), this translates to a value of $\beta = 4 \times 10^{-2} \text{ cm/MW}$. Catalano *et al.*⁵⁶ also performed similar measurements on high-purity monocrystals of KBr of size $6.5 \text{ mm} \times 5 \text{ mm} \times 1.5 \text{ mm}$. From the slope of the experimentally obtained curve, using a plot of the total induced charge Q as a function of the intensity I , they concluded that a two-photon process was responsible for the observed NLP and assigned a value less than 7.12 eV for the band gap of KBr, in good agreement with a value of 7.3 eV assigned earlier by Frohlich and Staginnus⁵⁷ based on two-photon spectroscopy. By contrast, single-photon optical absorption and intrinsic photoconductivity measurements at 80 K had previously incorrectly fixed this gap at 7.8 eV. Whereas the minimum energy gap of KBr is about 7.12 eV, corresponding to the transition $\Gamma_8^- \rightarrow \Gamma_6^+$, the larger value of 7.8 eV is the energy separation between the states Γ_6^- and Γ_6^+ , in agreement with the spin-orbit splitting of the valence band of KBr. This example illustrates the usefulness of MPA experiments in elucidating details of the band parameters of crystalline solids. The value of σ_2 for KBr at $0.266 \mu\text{m}$ deduced by Catalano *et al.* is $1.5 \times 10^{-50} \text{ cm}^4 \text{ sec}$ ($\beta = 1.45 \times 10^{-3} \text{ cm/MW}$).

Wenzel *et al.*⁵⁸ performed NLT experiments on 5.7-mm-thick disks of optical-quality Ge in the wavelength region $2.6\text{--}3.1 \mu\text{m}$ ($\omega = 0.477\text{--}0.4 \text{ eV}$) obtained from a HF laser operating multimode with a pulse duration of 100 nsec. A value of 2.5 cm/MW was deduced for β .

Gvazdzhadze *et al.*⁴³ found that there was virtually no absorption of $1.06\text{-}\mu\text{m}$ radiation for a pulse duration of 10^{-11}

sec in 0.2-cm-thick crystals of GaAs when the intensity was in the range of 0.05–2 GW/cm² at a temperature of 77 K. For intensities greater than 2 GW/cm², absorption did take place under the same conditions, but the nonlinear absorption coefficient was roughly 3 orders of magnitude smaller than the corresponding values obtained with nanosecond pulses of the same wavelength. On the other hand, at room temperature there was ordinary TPA at all intensities. The above observations were explained as the effects of coherent interactions, such as self-induced transparency.

Lee and Fan²³ measured the TPA coefficients of GaAs, InP, and ZnTe at 1.06 μm ($t_p = 30$ nsec, $P_{max} \sim 30$ MW) and of InSb at 10.6 μm ($t_p = 200$ nsec, $I \sim 3$ MW/cm²) by means of the NLT technique. Four samples of *n*-type GaAs single crystals with carrier concentrations 1×10^{14} , 2.2×10^{14} , 4×10^{14} , and 4×10^{16} /cm³ were used at room temperature. In addition, the sample thickness was varied from 0.15 to 0.25 cm. The measured values of β varied from 0.23 to 0.3 cm/MW. The sample with $n = 2.2 \times 10^{14}$ /cm³ and thickness 0.25 cm was found to have a value of $\beta = 0.17$ cm/MW at 15 K, as opposed to a value of 0.23 cm/MW at room temperature. Measurements were also made on a sample of undoped ZnTe single crystal with $p = 1 \times 10^{16}$ /cm³ in the temperature range 80–375 K. The value of β increased from 0.010 cm/MW at 150 K to 0.052 cm/MW at 375 K. There was no measurable TPA below 130 K. A single crystal of InP ($n = 10^{17}$ /cm³, thickness 0.577 cm) had a value of β in the range (0.18–0.21) ± 0.09 cm/MW, whereas two polycrystalline samples ($n = 1 \times 10^{16}$ and 2×10^{16} /cm³, thickness, 0.186 and 0.182 cm, respectively) gave β values of 0.2 ± 0.1 and 0.26 ± 0.13 cm/MW, respectively. Finally, a single crystal of InSb with $n = 3 \times 10^{14}$ /cm³ was found to have a TPA coefficient of 15 cm/MW at room temperature for 10.6-μm radiation.

Catalano *et al.*³⁸ conducted NLT, NLP, and NLL experiments on CdS single crystal with ruby laser pulses of duration 20 nsec and peak power 200 MW obtained from a Q-switched source. A value of 2.5×10^{-49} cm⁴ sec was obtained for the nonlinear cross section corresponding to an atomic density of 2×10^{22} atoms/cm³ ($\beta = 7.02 \times 10^{-2}$ cm/MW). They also conducted⁵⁹ NLT and NLP measurements on GaP monocrystals of several-millimeter dimensions using the same laser and found the nonlinear absorption cross section to be 1.2×10^{-48} cm⁴ sec ($\beta = 0.413$ cm/MW).

In other experiments, Bepko⁶⁰ studied the anisotropy of TPA in GaAs and CdTe at 1.064 μm at room temperature and at 85 K. As the angle of polarization vector of the incident radiation was changed with respect to the crystal axis, the TPA varied by ±15% at room temperature, with larger variations being observed at 85 K. Measured values of β were 0.072 cm/MW at 300 K and 0.080 cm/MW at 85 K, both for [111] normal incidence.

Grasyuk *et al.*^{61,62} investigated the TPA in *n*-type GaAs ($n = 10^{16}$ /cm³; thickness, 1.6 mm) at wavelengths of 1.064, 1.315, 1.415, and 1.650 μm that were obtained by high-efficiency frequency conversion of Nd:YAG laser radiation through stimulated Raman scattering. A maximum intensity of 20 MW/cm² was incident upon the sample, with the transmitted intensity measured by a calorimeter. The following numerical results were obtained: $\beta(1.65 \mu\text{m}) = 1.13 \pm 0.07$ cm/MW, $\beta(1.415 \mu\text{m}) = 0.2 \pm 0.04$ cm/MW, $\beta(1.315 \mu\text{m}) = 0.175 \pm 0.02$, and $\beta(1.064 \mu\text{m}) = 0.042 \pm 0.004$ cm/MW, respectively. These authors noted that β was a maximum when $2\hbar\omega \simeq E_g$

and monotonically decreased for $2\hbar\omega > E_g$; they attributed this behavior to the influence of deep level impurities.

Bechtel and Smith⁸² conducted NLT measurement on GaAs (doped with Te), CdTe, ZnTe, and CdSe, using 1.064-μm radiation with a FWHM pulse width of 30 ± 6 psec. In their analysis of the experimental data they took into consideration the effects of free-carrier absorption, second-harmonic generation, uniformity of the pulse, laser polarization, and crystal orientation. For GaAs they obtained the following results: A sample with thickness 0.09 cm and electron density 2×10^{18} /cm³ as well as a second sample of thickness 0.22 cm and electron concentration 5×10^{16} /cm³ yielded TPA coefficients of 0.03 ± 0.005 cm/MW when oriented for [110] normal incidence, with the laser polarized along the (001) direction. A third sample, 1.29 cm thick with $n = 5 \times 10^{16}$ /cm³, gave a lower value of β , viz., 0.023 ± 0.005 cm/MW, under the same conditions. This reduction was attributed to reflection effects. It was also noted that, for the third sample, β was 20% greater for the laser polarized along the [110] direction than for [001] polarization. A sample of *n*-type CdTe, 0.49 cm thick, oriented for [110] normal incidence and laser polarized along the [001] direction, had $\beta = 0.025 \pm 0.005$ cm/MW, whereas a *p*-type sample of ZnTe, 0.1 cm thick, had $\beta = 0.008 \pm 0.004$ cm/MW under the same conditions. Finally, a hexagonal CdSe sample 0.385 cm thick with laser incident along the crystalline *c* axis gave a value of $\beta = 0.030 \pm 0.005$ cm/MW.

In a particularly revealing set of experiments, Gibson *et al.*⁴¹ performed NLP measurements on *n*-type InSb and *n*-Ge crystals at room temperature and analyzed the experimental data by explicitly including FCA. A sample of InSb with $n = 6 \times 10^{16}$ /cm³ and dimensions 0.95 cm × 0.09 cm × 0.05 cm, when exposed to 23-nsec pulses from a mode-locked CO₂ laser, exhibited TPA with a coefficient of 0.1–0.3 cm/MW. These authors also measured the TPA coefficient of Ge with an HF laser whose wavelength varied from 2.6 to 3 μm and whose pulse duration was 480 nsec. The average value of β obtained from NLP experiments varied from 0.7 cm/MW at 2.6 μm to nearly zero at 3 μm. The above work showed that in both Ge and InSb the reduced transmission noted at high intensities was primarily due to absorption by the generated free carriers and was not due to intrinsic TPA itself. They also reinterpreted the experimental data of Lee and Fan²³ on InSb at 1.06 μm by including FCA in the analysis and deduced a value of 0.16 cm/MW for the TPA coefficient. This value, while in agreement with the experimental result of Gibson *et al.* above, is substantially different from the value of 15 cm/MW originally reported by Lee and Fan, who neglected FCA in their analysis. This example illustrates the significant role played by FCA in MPA experiments and can partially explain the large disparities among some experimentally determined coefficients.

Penzkofer and Falkenstein^{63,64} measured the TPA coefficient of rutile TiO₂ by means of NLT. A mode-locked Nd laser generated pulses of energy 3 mJ and duration 6 psec, which was converted into its second harmonic with 20% energy-conversation efficiency. The rutile crystal had a length of 1 cm, and its *c* axis was perpendicular to the light polarization and propagation directions. A value of 1.4×10^{-2} cm/MW was obtained for β . They also converted the second harmonic of a Nd laser to light at 0.626 μm by stimulated Raman scattering in a cell of ethyl alcohol and repeated the

NLT experiment. They found that β decreased from 1.4×10^{-2} cm/MW at $0.53 \mu\text{m}$ to 6.5×10^{-3} cm/MW at $0.626 \mu\text{m}$.

Zubarev *et al.*⁶⁵ conducted calorimetric measurements of the nonlinear transmission of nanosecond pulses of a Nd:YAG laser in three different samples of GaAs: a pure sample ($\beta = 0.078 \pm 0.005$ cm/MW), a sample with small amounts of O₂ impurity ($\beta = 0.035 \pm 0.003$ cm/MW), and a sample heavily doped with Cr impurity ($10^{17}/\text{cm}^3$). Whereas the normalized transmission coefficients of the first two samples decreased with increasing intensity, that of the third sample increased because of the saturation of the transitions from the deep level impurities. Adduci *et al.*⁶⁶ carried out NLT measurements on the layered compounds GaSe and PbI₂ with Nd and ruby lasers, respectively, and they obtained the following results: β (GaSe, $1.064 \mu\text{m}$) = 0.11 cm/MW and β (PbI₂, $0.694 \mu\text{m}$) = 0.25 cm/MW. Reintjes and Eckardt⁶⁷ made NLT measurements of the absolute TPA coefficients of KDP and ADP at $0.266 \mu\text{m}$, using laser pulses of duration 30 psec. Their theoretical analysis revealed that in general a Gaussian pulse gave a larger value of β than a square pulse. In order to eliminate this ambiguity resulting from pulse profile, they used apertured pulses in their experiment and obtained the following results: β (KDP) = $(2.7 \pm 0.7) \times 10^{-5}$ cm/MW and β (ADP) = $(11 \pm 3) \times 10^{-5}$ cm/MW.

Bosacchi *et al.*⁶⁸ measured the NLT of ultrashort pulses ($t_p = 9$ psec) of a Nd laser whose intensity was varied to as high as 30 GW/cm^2 , through GaAs wafers of thickness $430 \mu\text{m}$, with free-carrier concentration of about $4 \times 10^{16}/\text{cm}^3$. They obtained the lowest value of the TPA coefficient of GaAs ever reported for $1.064 \mu\text{m}$ radiation, namely, 0.015 cm/MW. Furthermore, their results were essentially the same at room temperature and liquid-nitrogen temperature, in contradiction to those of Gvardzhaladze *et al.*,⁴³ which showed sharp differences between the NLT data at the two temperatures.

Dempsey *et al.*⁶⁹ measured the NLT of *n*-InSb ($10^{14}/\text{cm}^3$) at 10, 77, and 293 K. The sample had a thickness of 0.106 mm , and laser pulses of wavelengths 9.6 and $10.6 \mu\text{m}$ were used. These authors pointed out that one probable reason for the widely different values of the nonlinear absorption coefficients obtained by different workers might have been the mixing of a number of axial modes in the lasers used. Evidently these authors used, in their experiment, laser pulses from a hybrid CO₂ laser giving single transverse and axial modes of high stability. They analyzed the experimental data numerically, employing a predictor-corrector algorithm based on Auger recombination, in which the free-carrier life time τ and TPA coefficient β were used as fitting parameters. The room-temperature data were consistent with a value of $\beta = 2.5$ cm/MW at $10.6 \mu\text{m}$ and $\beta = 8$ cm/MW at $9.6 \mu\text{m}$, with a value of $\tau = 32$ nsec in both cases.

Liu *et al.*^{70,71} measured the absolute TPA coefficients of UV-transmitting materials using well-calibrated single picosecond pulses ($t_p = 30$ psec) of the third and fourth harmonics of a mode-locked Nd:YAG laser and obtained the following results: At $0.355 \mu\text{m}$, RbBr, RbI, and KI had TPA coefficients in the range $(2.43 \times 10^{-3} - 7.29 \times 10^{-3})$ cm/MW, whereas KDA, KDP, RDA, RDP, and CDA had β values in the range $(5.4 \times 10^{-6} - 5.12 \times 10^{-5})$ cm/MW. At $0.266 \mu\text{m}$, RbCl, RbBr, RbI, NaCl, NaBr, KCl, KBr, and KI had β 's in the range $(1.02 \times 10^{-3} - 3.75 \times 10^{-3})$ cm/MW, whereas SiO₂, CaCO₃, KDP, ADP, and Al₂O₃ had β 's that were between 4.5×10^{-5} and 2.7×10^{-4} cm/MW. CdF₂ showed a dramatic

change in the TPA coefficient with change in frequency, rising from 4.17×10^{-5} cm/MW at $0.355 \mu\text{m}$ to 1.6×10^{-3} cm/MW at $0.266 \mu\text{m}$ —an increase of approximately 38-fold.

Bass *et al.*⁵⁰ measured the TPA in single crystals of CdSe and CdTe at room temperature for $1.06-\mu\text{m}$ laser pulses of duration 16 nsec by means of a laser calorimeter whose sensitivity was 1 part in 10^5 . They took into account reflections at the rear surface of the crystals and obtained the values of 0.13 ± 0.04 cm/MW for β in CdTe and 0.05 ± 0.014 cm/MW for the same quantity in CdSe. Stewart and Bass⁷² later extended these measurements to GaAs, CdS_{0.25}Se_{0.75}, and CdS_{0.5}Se_{0.5} and also to include $1.318-\mu\text{m}$ radiation. They noted that the TPA coefficient (at $1.064 \mu\text{m}$) increased with increasing pulse width.

On the other hand, Catalano and Cingolani^{73,74} measured the NLT of ruby and Nd lasers through ZnTe as a function of temperature between 77 and 400 K. The sample was *p* type with a hole concentration in excess of $10^{12}/\text{cm}^3$ and a thickness of 0.15 cm , and the laser pulses had a duration of 20 nsec and a peak intensity 200 MW/cm^2 . These authors used a single-channel method with 25% accuracy as well as a two-channel method (after Lotem and Lynch⁴⁸), which resulted in 10% accuracy of the measured TPA coefficient. They found that the exciton effects were important for two-photon energies close to the band gap but negligible well away from the band edge, in accordance with the findings of Lee and Fan.²³ The measured β of ZnTe varied from 0.035 cm/MW at $1.064 \mu\text{m}$ to 0.26 cm/MW at $0.694 \mu\text{m}$. Miller *et al.*⁴⁵ deduced the TPA coefficients of InSb and Hg_{0.78}Cd_{0.22}Te at wavelengths of 9.6 and $10.6 \mu\text{m}$ from NLT measurements by taking into account the effects of FCA. The InSb and Hg_{0.78}Cd_{0.22}Te samples had thicknesses of 106 and $370 \mu\text{m}$, respectively, whereas the 9.6 - and $10.6-\mu\text{m}$ lasers had peak intensities of 1.2 and 2.64 MW/cm^2 , respectively. The TPA coefficient of InSb ($n = 2.14 \times 10^{16}/\text{cm}^3$ at 77 K) was found to be $8 \text{ cm/MW} \pm 40\%$ at $10.6 \mu\text{m}$ and $14 \text{ cm/MW} \pm 40\%$ at $9.6 \mu\text{m}$ when the experimentally measured value of 28 nsec was used for the free-carrier lifetime in the above analysis. These authors noted that the value of β in InSb obtained by Gibson *et al.*,⁴¹ who used a similar analysis, was almost 2 orders of magnitude smaller. Miller *et al.* attributed this discrepancy to the large concentrations of free electrons ($>10^{17}/\text{cm}^3$) in the sample used by Gibson *et al.*, which might have resulted in significant band filling. For Hg_{0.78}Cd_{0.22}Te they assumed a value of 40 nsec for the lifetime of free carriers ($n = 8 \times 10^{15}/\text{cm}^3$) and found β at $10.6 \mu\text{m}$ to be 14 cm/MW .

Later, Johnston *et al.*⁷⁵ repeated the NLT and NLP measurements on the same sample of *n*-type InSb used by Miller *et al.*⁴⁵ and a different specimen of Hg_{0.78}Cd_{0.22}Te in the temperature range 77 – 300 K . An assumption different from that made earlier with regard to the free-carrier lifetime τ resulted in values of $\tau = 47$ nsec and $\beta = 4.8 \text{ cm/MW}$ from InSb at room temperature for the $10.6-\mu\text{m}$ laser radiation. At 77 K the value of β was an order of magnitude smaller, viz., 0.22 cm/MW , whereas the corresponding value of τ was 143 nsec. For Hg_{0.78}Cd_{0.22}Te they obtained β values of 10 cm/MW at 300 K and 30 cm/MW at 150 K . This experiment and analysis reveal the importance of properly taking into account the variations in physical parameters, such as band gap and carrier lifetime, with changes in temperature in experimental determinations of the nonlinear absorption coefficients. Miller and Ash⁷⁶ measured the TPA coefficients of

Table 1. Published Experimental Values of Direct TPA Coefficients

Crystal	Wavelength (μm)	β (cm/MW)	t_p	T (K)	Source
ADP	0.266	$2.7 \times 10^{-4} \pm 30\%$	30 psec	—	Liu et al. ⁷⁰
	0.266	$(11 \pm 3) \times 10^{-5}$	30 psec	—	Reintjes and Eckardt ⁶⁷
	0.355	$6.8 \times 10^{-6} \pm 35\%$	30 psec	—	Liu et al. ⁷⁰
AgGaSe ₂	1.064	1.4×10^{-3}	5–15 psec	10	Miller and Ash ⁷⁶
	0.266	$2.7 \times 10^{-4} \pm 30\%$	30 psec	—	Liu et al. ⁷⁰
Al ₂ O ₃	0.266	$2.4 \times 10^{-4} \pm 30\%$	30 psec	—	Liu et al. ⁷⁰
CaCO ₃	0.266	$1.6 \times 10^{-3} \pm 5\%$	30 psec	—	Liu et al. ⁷⁰
	0.355	$4.17 \times 10^{-5} \pm 15\%$	30 psec	—	Liu et al. ⁷⁰
CdS	0.694	1.4×10^{-2}	20 nsec	—	Cingolani et al. ⁸¹
		3.0×10^{-2}	30 nsec	—	Arsenev et al. ⁸⁵
		7.0×10^{-2}	20 nsec	300	Catalano et al. ³⁸
CdS _{0.25} Se _{0.75}	1.064	0.065 ± 0.020	11.4 nsec	300	Stewart and Bass ⁷²
	1.064	0.21 ± 0.063	26.4 nsec	300	Stewart and Bass ⁷²
CdS _{0.5} Se _{0.5}	1.064	0.032 ± 0.01	11.4 nsec	300	Stewart and Bass ⁷²
	1.064	0.135 ± 0.041	26.4 nsec	300	Stewart and Bass ⁷²
CdSe	1.064	0.03 ± 0.005	30 psec	300	Bechtel and Smith ⁸²
	1.064	0.05 ± 0.014	16 nsec	—	Bass et al. ⁵⁰
	1.064	0.2	20–100 nsec	300	Ralston and Chang ^{53,54}
CdTe	1.064	0.025 ± 0.008	11.4 nsec	300	Stewart and Bass ⁷²
		0.038 ± 0.011	26.4 nsec	300	Stewart and Bass ⁷²
		0.048 ± 0.014	27.6 nsec	300	Stewart and Bass ⁷²
	1.318	0.067 ± 0.020	79.2 nsec	300	Stewart and Bass ⁷²
	1.064	0.025 ± 0.0005	30 psec	300	Bechtel and Smith ⁸²
		0.037 ± 0.011	11.4 nsec	300	Stewart and Bass ⁷²
		0.046 ± 0.014	26.4 nsec	300	Stewart and Bass ⁷²
		0.053 ± 0.016	11.4 nsec	300	Stewart and Bass ⁷²
		0.078 ± 0.023	37.8 nsec	300	Stewart and Bass ⁷²
		0.13 ± 0.04	16 nsec	—	Bass et al. ⁵⁰
GaAs		0.14–0.22	—	85	Bepko ⁶⁰
		0.17–0.2	—	300	Bepko ⁶⁰
	1.318	0.120 ± 0.036	79.2 nsec	300	Stewart and Bass ⁷²
		0.135 ± 0.041	79.2 nsec	300	Stewart and Bass ⁷²
		0.2–0.3	20–1000 nsec	300	Ralston and Chang ^{53,54}
	1.064	0.015	8 psec	77,300	Bosacchi et al. ⁶⁸
		0.02	20–1000 psec	300	Ralston and Chang ^{53,54}
		0.028 ± 0.005	30 psec	300	Bechtel and Smith ⁸²
		0.030 ± 0.009	11.4 nsec	300	Stewart and Bass ⁷²
		0.042 ± 0.004	40–60 nsec	300	Grasyuk et al. ⁶²
GaP		0.078 ± 0.005	10 nsec	—	Zubarev et al. ⁶⁵
		0.072	—	300	Bepko ⁶⁰
		0.080	—	85	Bepko ⁶⁰
		0.2	100 nsec	—	Oksman et al. ⁸³
		0.23–0.30	30 nsec	300	Lee and Fan ²³
		0.3±0.05	40 nsec	77	Grasyuk et al. ⁸⁴
		0.36 ± 0.02	22 nsec	—	Lee and Fan ⁶
		0.8	30 nsec	—	Arsenev et al. ⁸⁵
		5.6	60 nsec	—	Jayaraman and Lee ⁸⁶
		9.0	40 nsec	77	Basov et al. ^{8,9}
GaS	1.318	0.033 ± 0.015	100–150 nsec	300	Kleinman et al. ³⁹
		0.175 ± 0.02	40–60 nsec	300	Grasyuk et al. ⁶²
	1.415	0.20 ± 0.04	40–60 nsec	300	Grasyuk et al. ⁶²
	1.65	1.13 ± 0.07	40–60 nsec	300	Grasyuk et al. ⁶²
	0.694	4×10^{-3}	50 nsec	77–300	Ashkinadze et al. ⁵¹
GaSe		0.413	20 nsec	80–300	Catalano et al. ⁸⁷
	0.694	0.1	—	300	Adduci et al. ⁶⁶
Ge	1.064	0.11	—	—	Adduci et al. ⁶⁶
	2.36	1.0	—	300	Zubov et al. ⁵²
	2.8	0.34	480 nsec	300	Gibson et al. ⁴¹
	2.8	2.5	100 nsec	—	Wenzel et al. ⁵⁸
	2.36	1.0	—	300	Zubov et al. ⁵²
	2.8	0.34	480 nsec	300	Gibson et al. ⁴¹
	2.8	2.5	100 nsec	—	Wenzel et al. ⁵⁸
Hg _{0.78} Cd _{0.22} Te	10.6	10	—	300	Johnston et al. ⁷⁵
		14.0	—	300	Miller et al. ⁴⁵
		30	—	150	Johnston et al. ⁷⁵

Table 1. Continued

Crystal	Wavelength (μm)	β (cm/MW)	t_p	T (K)	Source
InP	1.064	0.23–0.3	30 nsec	300	Lee and Fan ⁶
InSb	10.6	0.26 \pm 0.13	22 nsec	300	Lee and Fan ⁶
		0.2	200 nsec	300	Gibson et al. ⁴¹
		0.22	300 nsec	77	Johnston et al. ⁷⁵
		0.256	75–150 nsec	77	Fossum and Chang ⁸⁸
		0.57 \pm 0.15	300 nsec	90	Danishevskii et al. ⁴⁰
		2.5	nsec	300	Dempsey et al. ⁶⁹
		4.8	300 nsec	300	Johnston et al. ⁷⁵
		8.0	nsec	300	Miller et al. ⁴⁵
		15.0 \pm 2.0	200 nsec	300	Lee and Fan ⁶
		16.0 \pm 5.0	nsec	300	Dovjak et al. ⁸⁹
KBr	9.6	8.0	nsec	300	Dempsey et al. ⁶⁹
		14.0	nsec	300	Miller et al. ⁴⁵
KCl	0.266	1.45×10^{-3}	—	300	Catalano et al. ⁵⁶
KDP	0.266	$2.0 \times 10^{-3} \pm 30\%$	30 psec	—	Liu et al. ⁷⁰
		$1.7 \times 10^{-3} \pm 20\%$	30 psec	—	Liu et al. ⁷⁰
		$2.7 \times 10^{-3} \pm 30\%$	30 psec	—	Liu et al. ⁷⁰
KI	0.266	$(2.7 \pm 0.7) \times 10^{-5}$	30 psec	—	Reintjes and Eckardt ⁶⁷
		$(2.7 \times 10^{-4}) \pm 30\%$	30 psec	—	Liu et al. ⁷⁰
		$5.9 \times 10^{-6} \pm 35\%$	30 psec	—	Liu et al. ⁷⁰
		$3.75 \times 10^{-3} \pm 30\%$	30 psec	—	Liu et al. ⁷⁰
		$7.29 \times 10^{-3} \pm 20\%$	30 psec	—	Liu et al. ⁷⁰
NaBr	0.266	4.0×10^{-2}	—	300	Catalano et al. ⁵⁵
		$(2.5 \times 10^{-3}) \pm 15\%$	30 psec	—	Liu et al. ⁷⁰
NaCl	0.266	$3.5 \times 10^{-3} \pm 25\%$	30 psec	—	Liu et al. ⁷⁰
PbI ₂	0.694	0.25	—	—	Adduci et al. ⁶⁶
RbBr	0.266	$2.18 \times 10^{-3} \pm 20\%$	30 psec	—	Liu et al. ⁷⁰
		$2.43 \times 10^{-3} \pm 20\%$	30 psec	—	Liu et al. ⁷⁰
RbCl	0.266	$1.02 \times 10^{-3} \pm 15\%$	30 psec	—	Liu et al. ⁷⁰
		$1.26 \times 10^{-3} \pm 30\%$	30 psec	—	Liu et al. ⁷⁰
RbI	0.266	$2.49 \times 10^{-3} \pm 20\%$	30 psec	—	Liu et al. ⁷⁰
		$4.62 \times 10^{-3} \pm 20\%$	30 psec	—	Liu et al. ⁷⁰
		$5.08 \times 10^{-3} \pm 15\%$	30 psec	—	Liu et al. ⁷⁰
RDA	0.355	$4.99 \times 10^{-5} \pm 15\%$	30 psec	—	Liu et al. ⁷⁰
		5.9×10^{-6}	30 psec	—	Liu et al. ⁷⁰
SiO ₂	0.266	4.5×10^{-5}	30 psec	—	Liu et al. ⁷⁰
		1.4×10^{-2}	6 psec	—	Penzkofer and Falkenstein ⁶³
TiO ₂	0.530	6.5×10^{-3}	6 psec	—	Penzkofer and Falkenstein ⁶⁴
		0.04	30 nsec	—	Arsenev et al. ⁸⁵
ZnSe	0.694	0.26	20 nsec	77–400	Catalano and Cingolani ⁷³
		0.035	20 nsec	—	Catalano and Cingolani ⁷³
ZnTe	1.064	0.008 \pm 0.004	30 psec	300	Bechtel and Smith ⁸²
	1.064	0.010	30 nsec	150	Lee and Fan ²³
	1.064	0.052	30 nsec	375	Lee and Fan ²³

the chalcopyrite structured semiconductor AgGaSe₂ (direct gap, 1.83 eV) by means of NLT. Undoped crystals of dimensions 21 mm \times 16 mm \times 1.4 mm were kept at 10 K, and a 1.06- μm mode-locked Nd:glass laser was used. The pulses had a duration of 5–15 psec, and they were separated by 10-nsec intervals. Maximum energy used was 0.25 mJ, and β was measured to be 0.0014 cm/MW.

Nonlinear self-action is a complicated interaction that manifests itself in the form of both self-focusing and self-defocusing for different intensities⁷⁷ and can significantly influence the results of TPA experiments. After a series of experiments on II–VI semiconductors, Borshch et al.⁷⁷ concluded that the principal mechanism responsible for self-focusing is the nonlinear polarizability of the bound electrons, whereas self-defocusing is caused by the nonequilibrium free carriers generated by TPA. Recently Catalano and Cingolani⁷⁸ quantitatively evaluated the effect of nonlinear self-action on the absolute TPA coefficient measurements in CdS.

These authors noted that for a single-mode ruby laser beam from a Q-switched source ($t_p \sim 20$ nsec) passing through CdS single crystals, the beam diameter decreased for intensities greater than 1.2 MW/cm² because of self-focusing. However, for intensities greater than 3 MW/cm² the beam cross section slightly increased because of self-defocusing. When the self-action effect was taken into consideration in the evaluation of the experimental TPA coefficient, a value of 0.056 cm/MW was obtained. This is 20% less than the value of 0.07 cm/MW obtained when self-action is neglected. A value of 0.056 cm/MW was also obtained by Lotem and deAraujo,⁴⁹ who used the two-channel method mentioned earlier in this section. From this it is clear that in the single-channel methods the self-action effect must be taken into consideration for accurate determination of β . If this effect cannot be evaluated quantitatively, then it is preferable to use the two-channel method.

The frequency dependence of the TPA should shed more

light on the underlying mechanisms and should enable one to choose among the various theoretical models. However, as can be seen below, experimental work in this area is limited because of the scarcity of intense tunable-laser sources. Van der Ziel⁷⁹ was the first to study the variation of β with photon energy in GaAs. Thin films of GaAs (on GaAs substrates) prepared by liquid epitaxy were subjected to IR laser radiation from a temperature-tuned parametric oscillator. The combined energy of the two photons was varied from 1.4 to 1.75 eV, and measurements were repeated at 4 and 300 K. It was found that for $2\hbar\omega - E_g < 0.01$ eV, the two-photon transition rate was proportional to $(2\hbar\omega - E_g)^{1/2}$, characteristic of a-a transitions, whereas for $2\hbar\omega - E_g > 0.01$ eV it was proportional to $(2\hbar\omega - E_g)^{3/2}$, reminiscent of a-f transitions. A drawback of this experiment is that the spread in laser energy is not large enough. The frequency dependence of TPA in InSb and $Hg_{0.78}Cd_{0.22}Te$ was studied by Johnston *et al.*,⁷⁵ who utilized the 9.6- and 10.6- μm lines of a hybrid CO₂ laser ($t_p \sim 300$ nsec, $P \sim 300$ KW) and varied the energy gaps by controlling the temperature between 77 and 300 K. This procedure amounted to a variation of $2\hbar\omega/E_g$ between 1.04 and 1.76. They found that the values of β for both InSb and $Hg_{0.78}Cd_{0.22}Te$, when scaled by a factor of $1/n^2E_g^3$, n being the refractive index, monotonically increased with $\hbar\omega/E_g$. This was in good agreement with the nonparabolic model for a-f transitions²⁴ and in poor agreement with the Keldysh theory, which predicted an initial increase in β followed by a decrease at higher energies. In contrast with this finding of Johnston *et al.* is a more recent finding of Casalboni *et al.*⁸⁰ in the indirect-gap crystal AgCl. These authors found that β initially increased from 1.25×10^{-4} cm/MW for $\hbar\omega = 2.05$ eV to 8×10^{-4} cm/MW for $\hbar\omega = 2.2$ eV. However, for $\hbar\omega = 2.34$ eV it was approximately an order of magnitude smaller than at 2.05 eV.

Thus the available experimental data on the frequency dependence of the TPA coefficient are unfortunately too limited and too inconclusive. Experiments covering a wider range of frequencies are needed. In such experiments it is desirable to use dye lasers of tunable frequencies rather than to achieve energy-gap tuning by controlling the temperature, which might affect other physical parameters.

Before making a meaningful comparison between the theoretical predictions and experimental data, it is important to note the following. As was already mentioned, the experimentally deduced TPA coefficients are significantly affected by many variables, such as laser-pulse duration, peak power,

spatial and temporal coherence of the lasers, sample thickness and temperature, type and concentration of impurities and free carriers, and experimental technique and method of analysis employed. Most of the theoretical calculations are for intrinsic TPA in pure crystals at room temperature that assume that coherence effects, FCA, etc. are absent. Even though we list below all the published experimental data, only those relating to nanosecond pulses and room temperature in which coherence effects are normally absent will or should be used for comparison with theory. First, we study those materials for which the experimental data are unambiguous. This will enable us to judge the reliability of the predictions of the different theoretical formulations regarding the nonlinear absorption coefficients. This knowledge will enable us to understand better the experimental data in those crystals in which there is a larger scatter.

In Table 1 we have listed available experimental data relating to direct TPA in solids along with the pulse duration and temperature. Although we have made every effort to include most of the published results, especially the more-recent data, the list is by no means exhaustive.

In Table 2 we list results of different theoretical calculations for several zinc-blende-type semiconductors along with the experimental data to which these theories apply. Whereas the original Keldysh formula considered the transitions starting from the hh band only, the modified Keldysh formula²⁶ includes the transitions from the lh and split-off-hole bands also wherever these transitions are energetically possible. The original Basov formula used the hh and lh bands and assumed the energy bands to be parabolic. The modified Basov formula²⁶ includes the split-off-hole band also, and the energy bands are taken to be nonparabolic of the form described by Eq. (23).

On comparing the theoretical predictions with the experimental data we note the following. In general, the original Keldysh and Basov formulas give the smallest values; the modified Keldysh or Basov results are somewhat larger and are in good agreement with those of Lee and Fan. The band-structure calculations give the largest coefficients. Specifically, in the case of InP and ZnSe the band-structure calculations overestimate the TPA coefficients by a factor of approximately 2, whereas the other models underestimate the result. In CdTe, GaAs, and InSb there is considerable spread in the experimental data, and most of the theoretical predictions fall within the range of reported experimental results. However, based on the success of the band-structure calcu-

Table 2. Comparison of Theoretical and Experimental TPA Coefficients (cm/MW) at 300 K with Nanosecond Pulses in Zinc-Blende-Structure Semiconductors

Crystal	Wavelength (μm)	Theoretical Data						Experimental Data ^a
		Keldysh		Basov		Lee and Fan	Band-Structure	
		Original	Modified	Original	Modified	-	0.201	0.037–0.078 0.13 ± 0.04 0.2–0.3
CdTe	1.064	0.023	0.051	0.037	0.083	-	0.201	0.037–0.078 0.13 ± 0.04 0.2–0.3
GaAs	1.064	0.019	0.057	0.030	0.088	0.058	2.179	0.02–5.6
InP	1.064	0.026	0.080	0.038	0.161	0.096	0.351	0.23–0.3 0.26 ± 0.13
InSb	10.64	6.2	15.21	8.97	14.38	14.3	-	0.2–16
ZnSe	0.694	0.0064	0.018	0.009	0.019	-	0.081	0.04

^a The references to the experimental data are given in Table 1.

Table 3. Comparison of Theoretical and Experimental TPA Coefficients in Alkali Halide Crystals (cm/GW)

Crystal	Wavelength (μm)	Theoretical Data				Experimental Data ^a		
		Keldysh		Braunstein				
		Original	Modified	Original	Modified	Original	Modified	
NaCl	0.266	0.226	0.678	0.037	0.681	0.026	0.042	$3.5 \pm 25\%$
KCl	0.266	0.291	0.873	0.052	0.858	0.041	0.066	$1.7 \pm 20\%$
KBr	0.266	0.502	1.506	0.073	0.48	0.287	0.57	$2.7 \pm 30\%$
KI	0.266	0.802	2.406	0.080	1.086	0.567	1.74	$2.0 \pm 30\%$
	0.355	1.02	3.06	0.176	2.232	0.312	0.56	$3.75 \pm 20\%$
RbCl	0.266	0.344	1.032	0.028	0.183	0.092	0.162	$7.29 \pm 20\%$
RbI	0.266	0.655	1.965	0.037	0.852	0.457	1.38	$1.02 \pm 15\%$
	0.355	0.848	2.544	0.081	1.746	0.225	0.399	$1.26 \pm 30\%$
								$5.08 \pm 15\%$

^a Liu et al.^{70,71}

lations in the case of InP and ZnSe, we propose values of the order of 0.1 and 1 cm/MW for the TPA coefficients of CdTe and GaAs, respectively, at 1.064 μm. One reason for many of the experimental data to be much smaller than the values proposed here might be the increase in the effective energy gap of the crystal because of the dynamic Franz-Keldysh effect (see Subsection 2.A.2 and Section 4). Also, the saturations of the transitions that are due to band filling could be important in this respect.

In Table 3 we compare the theoretical results on alkali halides with the experimental data of Liu et al.^{70,71} measured with 30-psec pulses. The original Keldysh result is for transitions from a single valence band in the nonparabolic approximation; that of Basov is for two valence bands in the parabolic approximation. In the modified forms of these models, both the degeneracy (the highest valence bands in the alkali halides considered here are triply degenerate) and nonparabolicity are taken into account, as was explained earlier. The original Braunstein formulation considers a higher conduction band for the intermediate state and gives the smallest TPA coefficients. In its modified form,^{25,26} exciton states in the forbidden gap serve as the intermediate state, and the nonparabolicity and degeneracy of the bands are included, resulting in substantially larger TPA coefficients.

The band-structure calculation²⁸ uses second-order perturbation theory along with the band structure obtained from the empirical pseudopotential method. On comparing the theoretical predictions with the experimental data we note the following: The band-structure calculation gives larger values, in closer agreement with the experimentally measured coefficients, than those of the analytical models. Among the analytical formulas employed for quick calculations, the modified Keldysh gives the best results when the two-photon energy is close to the band gap, whereas the modified Basov results come closest to the experimental data for photon energies significantly different from the band-gap energy. This is not surprising because the leading term in the series expansion of the Keldysh formula corresponds to a-a transitions,²⁶ which are the most important transitions near the TPA edge, where the a-f transitions are extremely weak. As one moves away from the band gap, the a-f transition described by the Basov formula becomes more important than the a-a transition. This trend is also in agreement with the experimental observation of Van der Ziel⁷⁹ that β is propor-

tional to the one-half power of $2\hbar\omega - E_g$ when $2\hbar\omega - E_g$ is smaller than 0.01 eV, while it is proportional to the three-halves power for greater values of $2\hbar\omega - E_g$.

B. Indirect Transitions

In many crystalline solids of interest (for example, Ge, Si, GaP, GaS, and SiC) the maximum of the valence band and the minimum of the conduction band occur at different points in the Brillouin zone. In this case the TPA edge results from the absorption of two photons, accompanied by the simultaneous absorption or emission of a phonon. Since this is a third-order process, it is much weaker than the direct two-photon transition. It is also strongly temperature dependent because of the phonon occupation probability.

Interest in two-photon indirect transitions started when Ashkinadze et al.⁹⁰ observed for the first time luminescence spectra that were due to the recombination of electrons and holes created in undoped single crystals of GaP at 77 K using nanosecond pulses from a Nd:YAG laser. The minimum direct-energy gap of GaP at 77 K is 2.9 eV, and a direct transition resulting from the simultaneous absorption of two photons of a Nd laser, each of energy 1.17 eV, is energetically impossible. However, a phonon-assisted two-photon transition can take place from the valence-band maximum at the Γ point to the conduction-band minimum at the X point [$E_g(\Gamma_{15}^v - X_1^c) = 2.332$ eV at 77 K]. Also, direct absorption of three photons of a Nd:YAG laser is possible. Both of these processes could result in the luminescence observed by Ashkinadze et al., whose experiment was unable to distinguish between the above two contributions. In an attempt to resolve this problem, Ashkinadze et al. theoretically calculated the probabilities of indirect two-photon and direct three-photon transitions. Using third-order perturbation theory, and a two-band model in which the spin-orbit split-off valence band served as the intermediate state, they derived the following expression for the probability of two-photon indirect transition at low temperature, in which an acoustic phonon participated (see also Ref. 91):

$$\frac{W_2^i}{L^3} = \frac{3 \cdot 2^5}{\Pi} \left(\frac{m_{cx}}{m_v} \right)^{3/2} \left(\frac{I}{\hbar\omega} \right)^2 \frac{\mu V_0 G^2 \Delta_{xcv} e^4}{\epsilon_\infty c^2 \hbar^5 \omega^2} \Psi(\omega). \quad (34)$$

In Eq. (34)

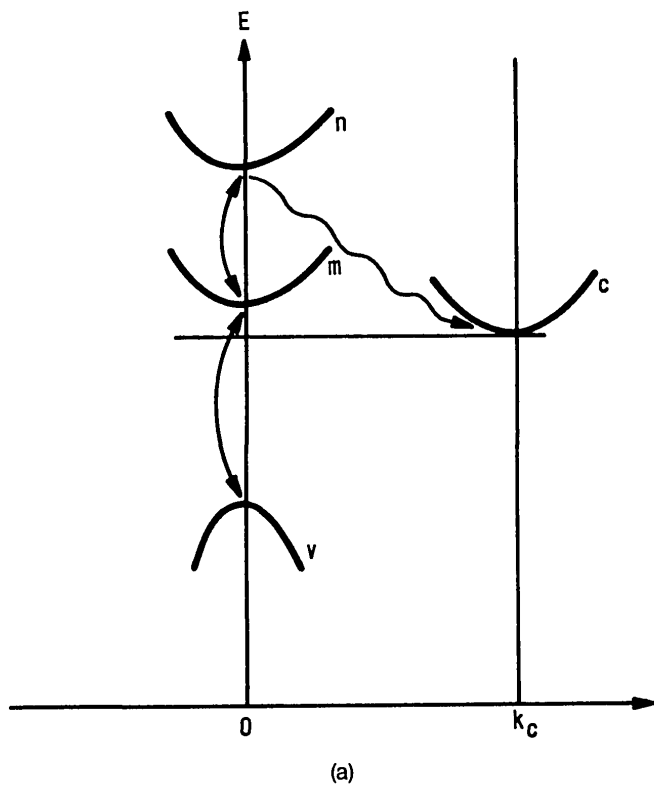
$$\Psi(\omega) = \int_0^\Gamma \frac{\sqrt{z}(\Gamma - z)^{3/2}}{(\Gamma_1 - z)^2(\Gamma_2 - z)^2} dz, \quad (35)$$

$$\Gamma = 2\hbar\omega - \Delta_{xcv} - \hbar V_l z_0, \quad (36)$$

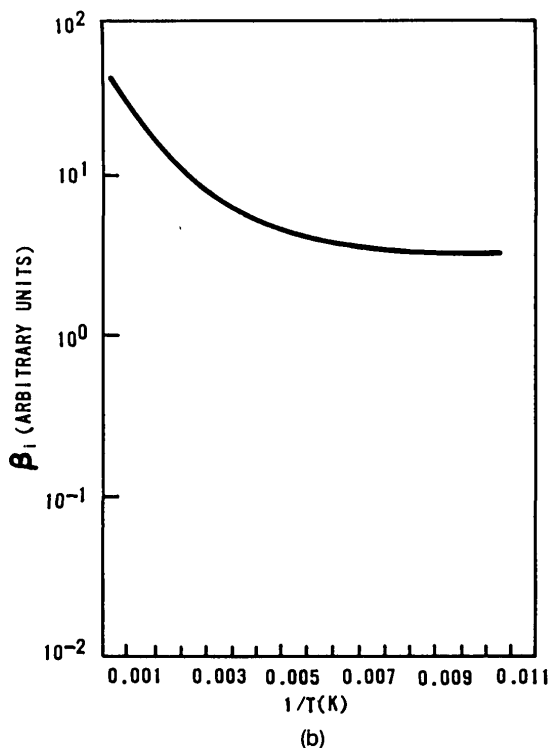
and

$$\tilde{\Gamma}_n = \Gamma + \frac{\mu}{m_v} (\Delta_{cv} - n\hbar\omega), \quad n = 1, 2, \quad (37)$$

where Δ_{xcv} is the energy separation $\Gamma_{15}^v - X_1^c$, Δ_{cv} is the energy separation $\Gamma_{15}^v - \Gamma_1^c$, V_l is the longitudinal sound velocity, z_0 is the phonon wave vector, $\mu^{-1} = m_c^{-1} + m_v^{-1}$,



(a)



(b)

Fig. 6. (a) Four-band model of Bassani and Hassan⁹⁵ for TPA in an indirect-gap crystal. (b) Temperature dependence of the indirect TPA coefficient of GaP at 1.064 μm ($\hbar\omega = 0.0447 \text{ eV}$) (after Bassani and Hassan⁹⁵).

m_{cx} is the conduction electron effective mass at X point, ϵ_∞ is the optical dielectric constant, G is the intervalley transition constant, and V_0 is the unit cell volume. For a Nd:YAG photon density of $3 \times 10^{15}/\text{cm}^3$, numerical calculations for GaP gave

$$W_2^i/L^3 \simeq 2.16 \times 10^{19} \text{ G}^2.$$

For $G \simeq 10 \text{ eV}$, Ashkinadze *et al.* obtained an absorption coefficient of $2 \times 10^{-5} \text{ cm}^{-1}$ ($\beta_i = 6.9 \times 10^{-6} \text{ cm/MW}$). At 0.694 μm the direct TPA coefficient in GaP obtained by the same authors is 0.1 cm^{-1} for an incident intensity of 50 MW/cm^2 ($\beta = 4 \times 10^{-3} \text{ cm/MW}$). Thus the theoretical indirect TPA coefficient is 3–4 orders of magnitude smaller than the direct TPA coefficient. By comparing the experimentally observed luminescence under the action of the Nd laser with that which is due to a ruby laser, these authors estimated that the indirect TPA at 1.064 μm was 4–5 orders of magnitude smaller than the direct TPA at 0.694 μm , in good agreement with their theoretical prediction.

Since then a number of workers have studied indirect TPA in GaP, GaAs, Si, etc., both theoretically and experimentally. Yee⁹² has presented theoretical calculations of the two-photon indirect transitions using a three-band model and including the effects of both optical and acoustical phonons. His final expression for allowed indirect TPA coefficient had the frequency dependence $(2\hbar\omega \pm \hbar\omega_p - E_g)^3$, whereas the corresponding forbidden transition had the dependence $(2\hbar\omega \pm \hbar\omega_p - E_g)^4$. Assuming that the deformation potentials of the valence and conduction bands of GaP were, respectively, 6 and 12 eV, Yee estimated the dipole-allowed TPA coefficient of GaP at 1.064 μm to be $2 \times 10^{-4} \text{ cm}^{-1}$ ($\beta_i = 8 \times 10^{-6} \text{ cm/MW}$) for optical-phonon-assisted transitions and $2 \times 10^{-3} \text{ cm}^{-1}$ ($\beta_i = 8 \times 10^{-5} \text{ cm/MW}$) for acoustic-phonon-assisted transitions for an incident intensity of 50 MW/cm^2 .

Later Yee and Chau⁹³ experimentally investigated the indirect TPA in n -type GaP ($e = 3 \times 10^{16}/\text{cm}^3$) by means of the NLT technique at room temperature with the help of a Q-switched Nd laser. The laser pulse had a duration of 50 nsec and maximum energy of 1J, and the GaP sample had a length of 0.5 to 1.5 cm. Their experiment yielded a value of $1.7 \times 10^{-3} \text{ cm/MW}$ for β_i for intensities between 40 and 400 MW/cm^2 . Revised calculations based on the model of Yee⁹⁴ yielded a value of $1.9 \times 10^{-4} \text{ cm/MW}$, an order of magnitude smaller than the experimentally measured β_i .

Bassani and Hassan⁹⁵ studied the problem of phonon-assisted TPA employing a four-band model [see Fig. 6(a)] in which all the transitions were dipole allowed. Their result was larger by 2 orders of magnitude than that of Kovarskii and Vitii,⁹¹ which corresponded to forbidden transition. Their final expression for a phonon-assisted two-photon transition rate is

$$W_2^i = \frac{8\pi e^4 A_0^4}{\hbar m^4 c^4} \sum_{m,n} \left[\left| \frac{Q_{cm} P_{mn} P_{nv}}{(E_m - E_v - 2\hbar\omega)(E_n - E_v - \hbar\omega)} \right. \right. \\ \left. \left. + \frac{P_{cm} Q_{mn} P_{nv}}{(E_m - E_v - \hbar\omega \pm \hbar\omega_p)(E_n - E_v - \hbar\omega)} \right. \right. \\ \left. \left. + \frac{P_{cm} P_{mn} Q_{nv}}{(E_m - E_v - \hbar\omega \pm \hbar\omega_p)(E_n - E_v \pm \hbar\omega_p)} \right| \right|^2 \\ \times \delta(E_c - E_v - 2\hbar\omega \pm \hbar\omega_p). \quad (38)$$

In Eq. (38), the P 's refer to electron–photon interaction and

Table 4. Indirect TPA Coefficients

Crystal	Wavelength (μm)	β_i (cm/MW)		Reference
		Experiment	Theory	
AgCl	0.53	10^{-5}		Casalboni <i>et al.</i> ⁸⁰
	0.62	1.25×10^{-4}		Casalboni <i>et al.</i> ⁸⁰
GaP	1.064		3.5×10^{-6}	Ashkinadze <i>et al.</i> ⁹⁰ and Kovarskii and Vitiu ⁹¹
			(77 K)	Bassani and Hassan ⁹⁵
			3.7×10^{-5}	(100 K)
			7.3×10^{-5}	(800 K)
		1.7×10^{-3}	1.9×10^{-4}	Yee and Chau ⁹³
		(300 K)	(300 K)	
		5.24×10^{-3}	4.49×10^{-4}	Catalano <i>et al.</i> ⁵⁹
		(300 K)	(300 K)	
		4.19×10^{-5}	3.2×10^{-6}	Catalano <i>et al.</i> ⁵⁹
		(80 K)	(80 K)	
GaS	1.064	$(2 \pm 1) \times 10^{-4}$		Bechtel and Smith ⁸²
		(300 K)		
Si	1.064	5×10^{-5}	1.7×10^{-5}	Adduci <i>et al.</i> ⁶⁶
			2.9×10^{-5}	Adduci <i>et al.</i> ⁶⁶
		1.9×10^{-3}		Reintjes and McGroddy ⁹⁹
		(20 K)		
	1.318	1.5×10^{-3}		Reintjes and McGroddy ⁹⁹
		(100 K)		
		0.021 ± 0.006		Stewart and Bass ⁷²

the Q 's refer to electron-phonon interaction. The photon and phonon frequencies are denoted by ω and ω_p , respectively. Bassani and Hassan noted that the anisotropies in the effective masses in general averaged out in the integration and did not produce qualitative differences. Using the band-structure scheme of Ge obtained earlier by Herman *et al.*⁹⁶ and that of GaP due to Cohen and Bergstresser²⁹ and Pollak *et al.*⁹⁷ in conjunction with group theoretical methods, they showed that in Ge only LO phonons could participate in the TPA process, whereas in GaP all except LO phonons were allowed. They also calculated the temperature dependence of β_i by including only the TO phonons that had the strongest interaction with photons. Using the phonon matrix elements obtained from the experimental one-photon indirect transition, they deduced the following values of β_i for GaP at $1.064 \mu\text{m}$ at different temperatures [see Fig. 6(b)]:

T (K)	β_i (cm $^{-1}$)	β_i (cm/MW)
<100	1.6×10^{-4}	2.8×10^{-5}
100	2.1×10^{-4}	3.7×10^{-5}
300	8.16×10^{-3}	1.4×10^{-3}
520	2.22×10^{-2}	3.9×10^{-3}
800	4.16×10^{-2}	7.3×10^{-3}

Hassan⁹⁸ extended the theory of phonon-assisted two-photon transitions in semiconductors to include the effects of excitons by assuming that excitons served the role of the final states. He used three different models in his calculations. First, he considered a four-band model that was analogous to Loudon's¹¹ three-band model for direct TPA. In this model the intermediate states were conduction-band states, whereas the final state was an s exciton. The second model was an extension of Mahan's^{12,13} model for direct TPA, and it consisted of two bands. The intermediate states were s and p excitons, and the final state was either an s or a d ex-

citon. Finally, Hassan considered a three-band model, in which the intermediate states were either one conduction band and one s exciton or two s excitons. The final state was always a p exciton. He found that the three-band model gave the largest value for the TPA coefficient, followed by the four- and two-band models. On comparing the TPA coefficients in the exciton and interband regions, Hassan found that the former was smaller by about 3 orders of magnitude than the latter. This he attributed to the exciton envelope function encountered in the former, which significantly reduced the absorption coefficient. Hassan also noted that the frequency and temperature dependences of the indirect TPA coefficient in the exciton region were similar to those for indirect one-photon transitions.

Reintjes and McGroddy⁹⁹ measured the indirect TPA coefficient of 1-cm-long undoped single crystals of Si at 20 and 100 K with the aid of a mode-locked Nd:glass laser and the NLT method. The crystal was oriented so that the laser beam was polarized along a [100] or a [110] direction, and no orientation dependence was observed. Picosecond pulses of 20-psec duration gave the following values of β_i : 1.9×10^{-3} cm/MW at 20 K and 1.5×10^{-3} cm/MW at 100 K.

Catalano *et al.*⁵⁹ carried out NLP measurements at 80 and 300 K on undoped monocrystals of GaP with a Q -switched Nd laser of 20-nsec pulse duration and several hundred megawatts of peak power, obtaining the following values for the nonlinear cross section for indirect TPA:

$$\sigma_2^i = 10^{-54} \text{ cm}^4 \text{ sec at } 300 \text{ K } (\beta_i = 2.14 \times 10^{-4} \text{ cm/MW}),$$

$$\sigma_2^i = 8 \times 10^{-53} \text{ cm}^4 \text{ sec at } 80 \text{ K } (\beta_i = 1.7 \times 10^{-6} \text{ cm/MW}).$$

Theoretical estimates based on the model of Bassani and Hassan⁹⁵ for allowed transitions yielded the following values:

$$\sigma_2^i = 2.1 \times 10^{-50} \text{ cm}^4 \text{ sec at } 300 \text{ K}$$

$$(\beta_i = 4.49 \times 10^{-4} \text{ cm/MW}),$$

$$\sigma_2^i = 1.5 \times 10^{-52} \text{ cm}^4 \text{ sec at } 80 \text{ K}$$

$$(\beta_i = 3.2 \times 10^{-6} \text{ cm/MW}),$$

and the models of Kovarskii and Vitiu⁹¹ and Yee^{92,94} gave considerably smaller values.

Bechtel and Smith⁸² conducted NLT measurements on crystalline GaP of thickness 4 mm, oriented for [111]-direction normal incidence of laser pulses from a Nd source, with an electric field along the [110] direction. The laser pulse had a FWHM of (30 ± 6) psec and a maximum intensity of 1 GW/cm². Assuming a free-hole absorption cross section of 2×10^{-17} cm², they deduced a value of $(2 \pm 1) \times 10^{-4}$ cm/MW for β_i of a GaP at 1.064 μm .

Adduci *et al.*⁶⁶ recently measured the indirect TPA cross section of GaS ($E_g^d = 2.8$ eV, $E_g^i = 2.3$ eV at 300 K) by NLP at Nd laser frequency ($\hbar\omega = 1.17$ eV). The sample used was a rectangular prism of dimensions 0.6 cm \times 0.6 cm \times 0.25 cm, and the laser pulses of duration 20 nsec and peak power 200 MW were produced by a Q-switched source. A value of 5×10^{-5} cm/MW was obtained for β_i , which agreed with the theoretical predictions of the models of Bassani and Hassan (1.7×10^{-5} cm/MW) and of Yee (2.9×10^{-5} cm/MW).

In Table 4 we summarize the available experimental and theoretical results relating to TPA in indirect-gap crystals.

3. THREE-PHOTON ABSORPTION

Three-photon absorption has been relatively less well studied than TPA because of the significantly smaller transition probabilities associated with it. In general, the n th-order transition probability varies as

$$W_n \sim \left(\frac{E_0}{E_x} \right)^{2n},$$

where E_0 is the electric-field amplitude of the incident radiation and E_x is the electric-field characteristic of the crystal (see Ref. 11). As a result of this, the higher-order multiphoton transition probabilities decrease rapidly with increasing order. In spite of this, there have been a few theoretical and experimental investigations of three-photon absorption in crystalline solids. In this section we briefly outline the salient features of these investigations.

Interest in three-photon absorption started when Ashkinadze *et al.*⁹⁰ observed NLL in GaP at 1.064 μm (see Subsection 2.B). As was pointed out earlier, their experiment was unable to clarify whether the observed luminescence was due to a direct three-photon transition or to an indirect two-photon transition. In order to shed more light on this situation, they calculated the theoretical probabilities of the above two processes. Employing third-order perturbation theory in conjunction with a two-band model, Ashkinadze *et al.*⁹⁰ derived the following expression for the direct three-photon absorption coefficient ($\gamma \equiv \alpha_3$):

$$\gamma = \frac{144\sqrt{2}\pi^2e^6(\bar{n}/L^3)^2|P_{cv}|^2}{\epsilon_\infty^{5/2}c\hbar^5\omega^7} \frac{|P_{cv}|^4}{m^2} \frac{1}{m^4} \mu^{3/2} (3\hbar\omega - E_g)^{1/2}$$

$$- \frac{4|P_{cv}|^2}{3m^2} \mu^{1/2} (3\hbar\omega - E_g)^{3/2} + \frac{4(3\hbar\omega - E_g)^{5/2}}{5\mu^{1/2}}. \quad (39)$$

For GaP with $\bar{n}/L^3 = 3 \times 10^{15}$ photons/cm³ and $\hbar\omega = 1.17$ eV, this formula gave a value of 10^{-5} cm⁻¹ for γ . Since this was of the same order of magnitude as the indirect TPA coefficient in GaP at 1.064 μm , Ashkinadze *et al.* concluded that probably

both these mechanisms competed in giving rise to the observed nonlinear luminescence.

Kovarskii and Perlin³⁵ later outlined a model calculation for multiphoton transitions of all orders (see Subsection 2.A.2). In the case of three-photon absorption, their result is

$$W_3 = \frac{\left(\frac{\bar{n}}{L^3}\right)^3 e^{6\pi^2} |P_{cv}|^2}{\sqrt{2}\omega^7 \epsilon_\infty^3 \hbar^5 \mu^{1/2} m^2} \left[\frac{4}{5} (3\hbar\omega - E_g)^{5/2} \right. \\ - \frac{2}{3} \frac{\mu}{m^2} (3\hbar\omega - E_g)^{3/2} (\hbar\omega) \left(\frac{|P_{cv}|^2}{\hbar\omega} + \frac{2|P_{cc'}|^2}{E_{cc'} - \hbar\omega} \right) \\ \left. + \frac{1}{4} \frac{\mu^2}{m^2} (3\hbar\omega - E_g)^{1/2} (\hbar\omega)^2 \left(\frac{|P_{cv}|^2}{\hbar\omega} + \frac{2|P_{cc'}|^2}{E_{cc'} - \hbar\omega} \right)^2 \right], \quad (40)$$

where $E_{cc'} = E_c - E_{c'}$. This formula also gave a value of $\gamma = 10^{-5}$ cm⁻¹ for GaP at 1.064 μm for $n/L^3 = 10^{16}$ /cm³. The general theory of MPA developed by Keldysh is also applicable for the case of three-photon absorption, and it often has been used to calculate the appropriate transition probabilities. The leading term of the three-photon absorption coefficient resulting from the Keldysh formula also has a one-half power dependence of $(3\hbar\omega - E_g)$, i.e., $\gamma \sim (3\hbar\omega - E_g)^{1/2}$.

Bobrysheva and Moskalenko¹⁰⁰ carried out calculations of the three-photon absorption in semiconductors by use of an S-matrix and second quantization formalism along with a two-band model. Their final formula is

$$\gamma = \frac{144\sqrt{2}\pi^2e^6}{c\epsilon_\infty^{5/2}\hbar^5\omega^7\sqrt{\mu}} \left(\frac{\bar{n}^3}{L^3} \right) \frac{B^2}{M^2} \left[\frac{4}{5} (3\hbar\omega - E_g)^{5/2} \right. \\ \left. + \frac{B^4}{M^4} \frac{\mu^2}{4} (3\hbar\omega - E_g)^{1/2} - \frac{2}{3} \frac{B^2}{M^2} \mu (3\hbar\omega - E_g)^{3/2} \right], \quad (41)$$

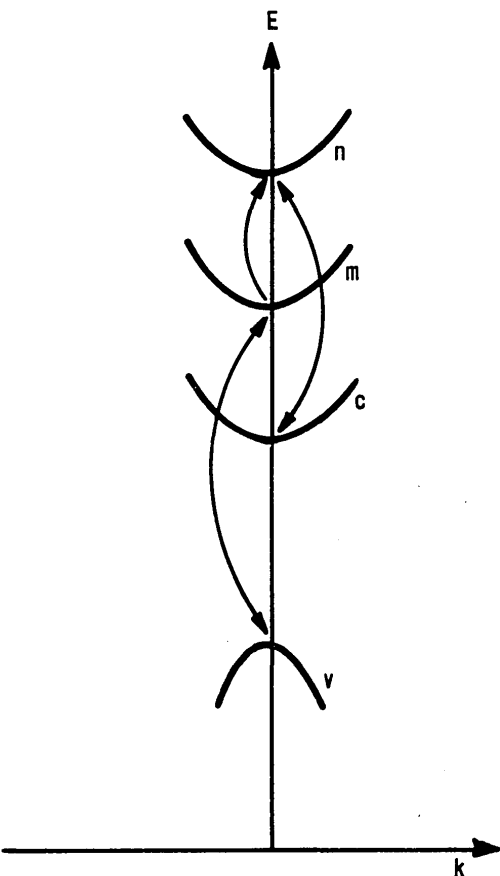


Fig. 7. Four-band model of Bassani and Hassan⁹⁵ for three-photon absorption in a direct-gap crystal.

where

$$B = M / \frac{3}{4} \frac{E_g}{\mu}. \quad (42)$$

For GaP they estimated a value of $1.5 \times 10^{-5} \text{ cm}^{-1}$ for γ at $1.064 \mu\text{m}$ when \bar{n}/L^3 was set equal to $10^{16}/\text{cm}^3$. These authors also discussed the selection rules and frequency and angular dependences of the three-photon absorption coefficient. They obtained the following frequency dependence for different types of three-photon transition:

$$\begin{aligned} \gamma &\sim (3\hbar\omega - E_g)^{1/2} && \text{for a-a-a transitions,} \\ \gamma &\sim (3\hbar\omega - E_g)^{3/2} && \text{for a-a-f transitions,} \\ \gamma &\sim (3\hbar\omega - E_g)^{5/2} && \text{for a-f-f transitions,} \\ \gamma &\sim (3\hbar\omega - E_g)^{7/2} && \text{for f-f-f transitions.} \end{aligned}$$

Bassani and Hassan⁹⁵ also developed a formula for direct three-photon absorption by means of third-order perturbation theory. They, however, used a four-band model (Fig. 7) that consisted of one valence band and three conduction bands, and all the four-energy bands were assumed to be parabolic functions of the wave vector:

$$\begin{aligned} E_v &= \alpha_v k^2, & E_n &= \Delta_n + \alpha_n k^2, \\ E_m &= \Delta_m + \alpha_m k^2, & E_c &= E_g + \alpha_c k^2. \end{aligned} \quad (43)$$

In Eqs. (43) the α 's refer to the inverse effective masses of the bands and Δ_n , Δ_m , and E_g are the minimum energy separations of bands n , m , and c , respectively, from the valence band v . Their final expression for the three-photon absorption coefficient is

$$\gamma = \frac{192\pi^2\hbar^2e^6N^2(3\hbar\omega - E_g)^{1/2}}{\epsilon_\infty^{5/2}m^6c\omega^3(\alpha_c + \alpha_v)^{3/2}} \left| \frac{P_{cm}P_{mn}P_{nv}}{\left[\Delta_n - \hbar\omega + \left(\frac{\alpha_v + \alpha_n}{\alpha_v + \alpha_c} \right) (3\hbar\omega - E_g) \right] \left[\Delta_m - 2\hbar\omega + \left(\frac{\alpha_v + \alpha_m}{\alpha_v + \alpha_c} \right) (3\hbar\omega - E_g) \right]} \right|^2. \quad (44)$$

Their numerical calculation showed that for GaP the direct three-photon absorption at $1.064 \mu\text{m}$ was 2 orders of magnitude smaller than the indirect two-photon transition at the same frequency and intensity.

Yee^{92,94} extended the formula for three-photon absorption within the context of a four-band model by using Kane's wave functions. He considered one conduction band and three valence bands and included intraband transitions as well as interband transitions. Furthermore, Yee treated the electron and hole effective masses as anisotropic tensors, which resulted in complicated angular dependence of the three-photon absorption. His final expression for the three-photon absorption coefficient is quite complicated because of the numerous intermediate states involved and will not be given here. Yee assumed that the cubic crystalline model was a good approximation for CdS and estimated the three-photon absorption coefficient of the crystal to be $5 \times 10^{-3} \text{ cm}^{-1}$ for radiation of wavelength $1.064 \mu\text{m}$ and intensity 20 MW/cm^2 ($\gamma = 12.5 \text{ cm}^3/\text{GW}^2$). Recently Mitra *et al.*¹⁰¹ calculated the three-photon absorption coefficients of several direct-gap crystals by means of a four-band model, in which the higher conduction bands served as the intermediate states. They considered both parabolic and nonparabolic band structures and found that the frequency dependence of the three-photon absorption coefficient was similar to that obtained from the Keldysh formula.

On the experimental side, Ashkinadze *et al.*¹⁰² were the first to detect three-photon absorption in a direct-gap semiconductor. They detected three-photon absorption of Nd laser light in CdS by means of the subsequent nonlinear luminescence at 4.2 K . They also used Nd and ruby lasers separately to produce luminescent radiation of the same intensity from three- and two-photon absorptions, respectively, and used this information along with the known TPA coefficient at $0.694 \mu\text{m}$ to deduce the three-photon absorption coefficient at $1.064 \mu\text{m}$. Assuming equal quantum efficiencies at the above two wavelengths, they obtained the relation

$$\frac{\beta I_{\text{ruby}}}{2\hbar w_{\text{ruby}}} = \frac{\gamma I_{\text{Nd}}}{3\hbar w_{\text{Nd}}}, \quad (45)$$

where the I 's refer to the two incident radiation intensities for the same luminescent intensity. Using the previously determined experimental value of 0.1 cm^{-1} for β at 50 MW/cm^2 , they estimated γ to be 10^{-6} – 10^{-5} cm^{-1} at the same intensity ($\gamma = 4 \times 10^{-4}$ – $4 \times 10^{-3} \text{ cm}^3/\text{GW}^2$). Arsenev *et al.*¹⁰³ measured γ in CdS at $1.064 \mu\text{m}$ by means of NLL. The laser pulses were obtained from a mode-locked Nd source and had a peak intensity of 20 GW/cm^2 and a duration of 3 psec . Their experiment gave a value of $2 \times 10^{-2} \text{ cm}^3/\text{GW}^2$ for γ . Jayaraman and Lee⁸⁶ also measured γ of CdS at $1.064 \mu\text{m}$, using picosecond pulses of maximum intensity of a few gigawatts per square centimeter from a Q-switched source. They, however, used the NLP technique and obtained a value of $1.3 \times 10^{-2} \text{ cm}^3/\text{GW}^2$. Catalano *et al.*⁸⁷ measured the three-photon absorption cross section of undoped CdS single crystals at 80 K for $1.064 \mu\text{m}$ by the NLL method. Their analysis

was similar to that employed earlier by Ashkinadze *et al.*¹⁰⁴ Peak powers of the ruby and Nd lasers were 200 and 100 MW , respectively, and both pulses had durations of 20 nsec . Using the previously measured value of $2 \times 10^{-49} \text{ cm}^4 \text{ sec}$ for σ_2 (ruby), they estimated σ_3 (Nd) to be $10^{-79} \text{ cm}^6 \text{ sec}^2$ ($\gamma = 5.7 \times 10^{-2} \text{ cm}^3/\text{GW}^2$). Catalano *et al.*⁵⁹ also measured the three-photon absorption cross section of GaP at $1.064 \mu\text{m}$ to be $6 \times 10^{-80} \text{ cm}^6 \text{ sec}^2$ ($\gamma = 4.2 \times 10^{-2} \text{ cm}^3/\text{GW}^2$). Catalano and Cingolani⁷³ later repeated the earlier experiment of Catalano *et al.*⁸⁷ on CdS by taking much care in reducing the influence of the nonuniformity of the beams on the three-photon absorption coefficient. In this experiment both the ruby and Nd lasers had peak powers of 100 MW , and the resulting value of γ for CdS at $1.064 \mu\text{m}$ was $(1.5 \pm 0.4) \times 10^{-2} \text{ cm}^3/\text{GW}^2$, smaller than the earlier result by a factor of approximately 4 . They also extended the measurement to PbI₂ and obtained a value of $(1 \pm 0.3) \times 10^{-2} \text{ cm}^3/\text{GW}^2$ for its three-photon absorption coefficient at $1.064 \mu\text{m}$. Penzkofer and Falkenstein⁶⁴ measured the room-temperature three-photon absorption coefficient of CdS at $1.064 \mu\text{m}$ by means of the nonlinear transmission of laser pulses of 6-nsec duration. The crystalline c axis was oriented normal to the propagation direction and the direction of polarization of the laser. These authors took into account free-carrier absorption in their analysis of the experimental data and obtained a value of $(1.1 \pm 0.3) \times 10^{-2} \text{ cm}^3/\text{GW}^2$ for the three-photon absorption coefficient.

Three-photon absorption has also been observed in several alkali halides and other dielectrics. Dneprovskii *et al.*¹⁰⁵ were the first to detect experimentally the simultaneous absorption of three photons of ruby laser light in pure single crystals of Al_2O_3 . They deduced the three-photon absorption coefficient of Al_2O_3 at $0.694 \mu\text{m}$ to be $0.1 \text{ cm}^3/\text{GW}^2$. Aseev *et al.*¹⁰⁶ have studied the three-photon absorption of ruby laser pulses of duration $0.5\text{--}2 \text{ nsec}$ in KI by means of the nonlinear photoconductivity. They estimated that 1.5×10^9 electrons were excited into the conduction band when the incident flux density of photons was $10^{24}/\text{cm}^2 \text{ sec}$. From this a value of $1.77 \times 10^{-3} \text{ cm}^3/\text{GW}^2$ for γ is calculated. Catalano *et al.*⁵⁵ conducted NLP measurements at room temperature on single crystals of NaCl with the second harmonic of ruby laser. They obtained a value of $(1 \pm 0.3) \times 10^{-80} \text{ cm}^6 \text{ sec}^2$ for the three-photon absorption cross section, which corresponds to a value of $6.9 \times 10^{-4} \text{ cm}^3/\text{GW}^2$ for γ . They also noted that the theoretical estimates based on the formula of Bassani and Hassan⁹⁵ gave a value of $2.6 \times 10^{-80} \text{ cm}^6 \text{ sec}^2$, which translates to a value of $1.8 \times 10^{-3} \text{ cm}^3/\text{GW}^2$ for γ .

Table 5 lists the available theoretical and experimental data relating to three-photon absorption in crystalline solids.

Ivchenko and Perlin¹⁰⁸ theoretically studied the polarization dependence of many-photon absorption in cubic crystals. They noted that in a two-band model MPA of order $2n + 1$, ($n > 0$) was forbidden at $k = 0$ for circular polarization, whereas it was allowed for linear polarization. Away from the zone center, the absorption of circularly polarized radiation had nonvanishing probability, but it was much smaller than that of linear polarization. They also noted that allowance for the contribution of other energy bands altered these results. Experimental studies of polarization dependence of MPA phenomena enable one not only to identify the actual processes involved but also to obtain information about the symmetry of wave functions and the positions of higher conduction bands and deeper valence bands.

Arifzhanov and Ivchenko²⁰ derived an expression for the linear-circular dichroism (LCD) for the three-photon absorption [$\text{LCD} = W^{(3)} \text{ linear}/W^{(3)} \text{ circular}$] within the context of a three-band model, valid for $3\hbar\omega - E_g \ll \hbar\omega$. Danishevskii *et al.*¹⁰⁹ carried out nonlinear photoconductivity experiments on InAs ($n = 2.3 \times 10^{16}/\text{cm}^3$) at 300 K with the 9.5- and $10.6-\mu\text{m}$ radiations from a Q-switched CO_2 laser. From the measured photoconductivity ratio, they deduced values of 27 and 1.4 for the LCD at 10.6 and $9.5 \mu\text{m}$, respectively. An increase in the crystal temperature from 299 to 325C altered the LCD from 27 to 2 for $10.6 \mu\text{m}$, whereas the LCD at $9.5 \mu\text{m}$ varied much less. This behavior is due to the temperature dependence of E_g and the strong dependence of LCD on $(3\hbar\omega - E_g)$ near the absorption edge.

The most complete treatment of the theoretical and experimental state of the art of LCD is contained in a recent paper by Arifzhanov *et al.*¹⁰⁹ They noted that the earlier theoretical results were too limited in scope, because they assumed that $3\hbar\omega - E_g \ll \hbar\omega$, which restricted their applicability to the absorption edge and its immediate vicinity, and were unable to explain the observed temperature dependence of LCD. Hence these authors set out to calculate $W_l^{(3)}$ and $W_c^{(3)}$ for arbitrary values of $3\hbar\omega - E_g$, experimentally investigate the frequency dependence of the three-photon absorption and LCD in InAs, and compare the results to assess the relative contributions of various types of transition involved in the three-photon absorption process. They noted that the two-band model was sufficient to calculate the three-photon absorption probabilities, since the contribution from the higher conduction band was much smaller. In the two-band model, a-f-f transitions of the type $vvvc$, $vucc$, $vccc$ can also contribute to the three-photon absorption for both linear and circular polarization. The role of these transitions becomes important as $3\hbar\omega - E_g$ increases, resulting in a decrease in LCD as one moves away from the absorption edge. Arifzhanov *et al.* employed the nonparabolic Kane model of

Table 5. Three-Photon Absorption Coefficients in Crystalline Solids

Crystal	Wavelength (μm)	γ (cm^3/GW^2)		Reference
		Experiment	Theory	
Al_2O_3	0.694	0.1		Dneprovskii <i>et al.</i> ¹⁰⁵
CdS	1.064	$4 \times 10^{-4} - 4 \times 10^{-3}$ $(1.1 \pm 0.3) \times 10^{-2}$ $(1.3 - 4) \times 10^{-2}$ $(1.5 \pm 0.4) \times 10^{-2}$ 2×10^{-2} 5.7×10^{-2}		Ashkinadze <i>et al.</i> ¹⁰² Penzkofer and Falkenstein ⁶⁴ Jayaraman and Lee ⁸⁶ Catalano and Cingolani ⁷⁴ Arsenev <i>et al.</i> ⁸⁵ Catalano <i>et al.</i> ³⁸ Keldysh ²⁸ Mitra <i>et al.</i> ¹⁰¹
GaP	1.064	4.2×10^{-2}	1.8×10^{-3} 8.2×10^{-3} (parabolic bands) 1.57×10^{-2} (nonparabolic bands) 2×10^{-2} 12.5	Bassani and Hassan ⁹⁵ Yee ⁹² Catalano <i>et al.</i> ³⁸ Kovarskii and Perlin ³⁴ Bobrysheva and Moskalenko ¹⁰⁰ Bassani and Hassan ⁹⁵ Ashkinadze <i>et al.</i> ¹⁰⁷
KI	0.694	1.77×10^{-3}		Aseev <i>et al.</i> ¹⁰⁶
NaCl	0.397	6.9×10^{-4}		Catalano <i>et al.</i> ⁵⁵
			1.8×10^{-3}	Bassani and Hassan ⁹⁵

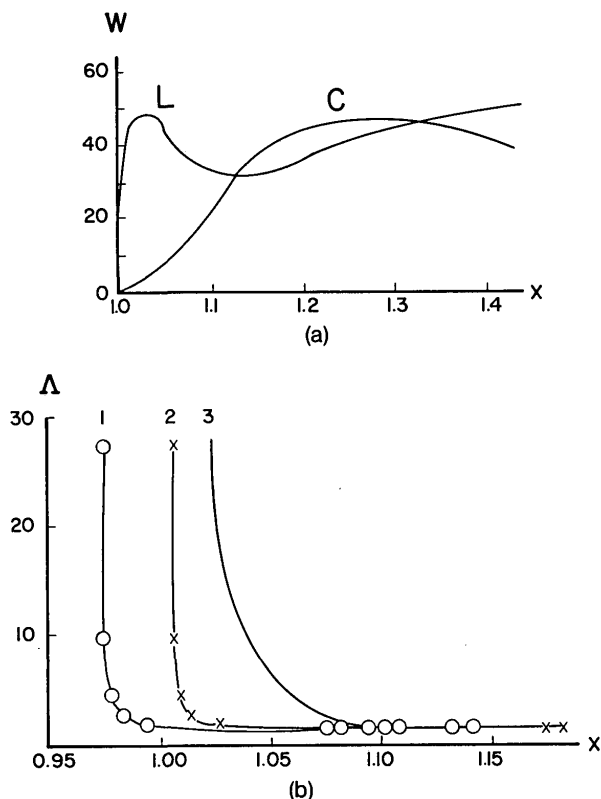


Fig. 8. (a) Dependence of the three-photon absorption probability W (in arbitrary units) for InAs calculated in the two-band model for linear (L) and circular (C) polarizations on the dimensionless parameter $x \equiv 3\hbar\omega/E_g$ (after Arifzhanov *et al.*¹¹⁰). (b) Dependence of the linear-circular dichroism (Δ) associated with three-photon absorption in InAs on the parameter $x \equiv 3\hbar\omega/E_g$. Curve 1 was deduced from the measured photoconductivity data assuming that $\partial E_g/\partial T = 2.8 \times 10^{-4}$ eV/deg. Curve 2 was obtained from the same experimental data assuming that $\partial E_g/\partial T = 2.46 \times 10^{-4}$ eV/deg. Curve 3 was obtained from the theoretical predictions for the three-photon transition probabilities assuming that E_g (0 deg) is 0.434 eV (after Arifzhanov *et al.*¹¹⁰).

band structure to calculate $W_l^{(3)}$ and $W_c^{(3)}$ for arbitrary $3\hbar\omega - E_g$ in InAs whose results are shown in Fig. 8(a). The non-monotonic nature of the dependence of $W^{(3)}$ is noteworthy.

Arifzhanov *et al.* also experimentally measured the nonlinear photoconductivity of n -type InAs ($n = 1.5 \times 10^{16}/\text{cm}^3$) with the 9.2-, 9.5-, 10.2- and 10.6- μm lines from a CO₂ laser. The experimental dependence of $W^{(3)}$ on $\hbar\omega$ agreed well with the theoretical predictions. The temperature dependence of LCD was studied by varying the temperature between 298 and 370 K at 9.5- and 10.6 μm wavelengths. The experimental data fell nicely on a monotonic curve [see Fig. 8(b)]. As predicted by theory, near the three-photon absorption edge the LCD fell sharply with increasing $\hbar\omega$ and then decreased smoothly to unity.

Most recently, Hassan and Raouff¹¹¹ have developed expressions for the polarization dependence of three-photon absorption in solids using the Wigner-Eckart theories for finite symmetry groups. However, no comparison with experimental data is presented in this work.

4. FOURTH- AND HIGHER-ORDER MULTIPHOTON ABSORPTIONS

Experimental and theoretical studies of MPA processes of order higher than three are limited in number for two main

reasons. The transition probabilities associated with these processes are extremely small, which makes the measurements difficult, if not impossible, to perform. Theoretical calculations are also quite cumbersome because of the numerous intermediate states involved. In spite of these difficulties, there have been a few investigations of these highly nonlinear absorption processes, which are briefly reviewed here.

Yee¹¹² derived an expression for the four-photon transition probability in semiconductors by employing fourth-order time-dependent perturbation theory along with Hartree and Hartree-Fock wave functions. For ZnS his calculation predicted an electronic transition probability rate of $10^{18}/\text{cm}^3 \text{ sec}$ owing to the simultaneous absorption of four photons from a ruby laser of peak intensity 100 MW/cm^2 . An estimate based on the Keldysh formula yields a value of $10^{16}/\text{cm}^3 \text{ sec}$ under identical conditions.

Dneprovskii *et al.*¹⁰⁵ observed the five-photon absorption of ruby laser in NaCl, which resulted in transitions to the excitonic levels. From the measured photocharge of $5 \times 10^{-12} \text{ C}$ at an incident intensity of 100 MW/cm^2 , they deduced a value of $8 \times 10^{-5} \text{ sec}^{-1}$ for the five-photon transition probability. The formula of Keldysh predicts that a much higher intensity, viz., 6 GW/cm^2 , is needed in order to obtain the measured photocharge. Aseev *et al.*¹⁰⁶ investigated the photoconductivity of NaCl, KCl, KBr, NaBr, and KI under illumination by ruby and Nd lasers. The energy of each laser was varied from 0.1 to 10 J, and the pulse duration varied over the range 0.5–2 msec. With a ruby laser, NaCl, KCl, and NaBr exhibited four-photon absorption, whereas with a Nd laser the first three crystals showed six-photon absorption and NaBr had a five-photon absorption. They found that the efficiency of each higher-order process was smaller than that of the preceding lower-order process by 1 or 2 orders of magnitude.

Catalano *et al.*^{55,56} conducted NLP measurements on color-center-free single crystals of NaCl, KCl, KBr, and KI using a ruby laser from a Q-switched source. The laser pulses had a duration of 20 nsec and a peak power of 200 MW; the crystalline samples were typically $0.8 \text{ cm} \times 2 \text{ cm} \times 1 \text{ cm}$ in dimensions. They obtained the following values for the nonlinear absorption cross sections:

$$\begin{aligned}\sigma_4(\text{KBr}) &= 2 \times 10^{-114} \text{ cm}^8 \text{ sec}^3, \\ \sigma_4(\text{KI}) &= (2 \pm 0.8) \times 10^{-114} \text{ cm}^8 \text{ sec}^3, \\ \sigma_5(\text{KCl}) &= (2.4 \pm 1.2) \times 10^{-140} \text{ cm}^{10} \text{ sec}^4, \\ \sigma_5(\text{NaCl}) &= (1.8 \pm 0.9) \times 10^{-140} \text{ cm}^{10} \text{ sec}^4.\end{aligned}$$

Theoretical estimates based on the formula of Yee^{92,94} gave a four-photon absorption cross section for KI of $6.8 \times 10^{-114} \text{ cm}^8 \text{ sec}^3$, in good agreement with the experimental value above.

We conclude this section with a rather interesting experimental observation made by Pyshkin *et al.*¹¹³ These authors investigated the density of free carriers generated by ruby laser pulses of duration 35 nsec from a Q-switched source, incident upon high-quality platelets of GaP. On increasing the intensity of the laser continuously from 10^{25} to 5×10^{27} photons/ $\text{cm}^2 \text{ sec}$, they noted the following: The generated carrier density (Δn) initially increased as I , because of impurity absorption, and then as I^2 , because of two-photon absorption; at higher intensities Δn was proportional to I^3 , suggestive of three-photon absorption; at even higher inten-

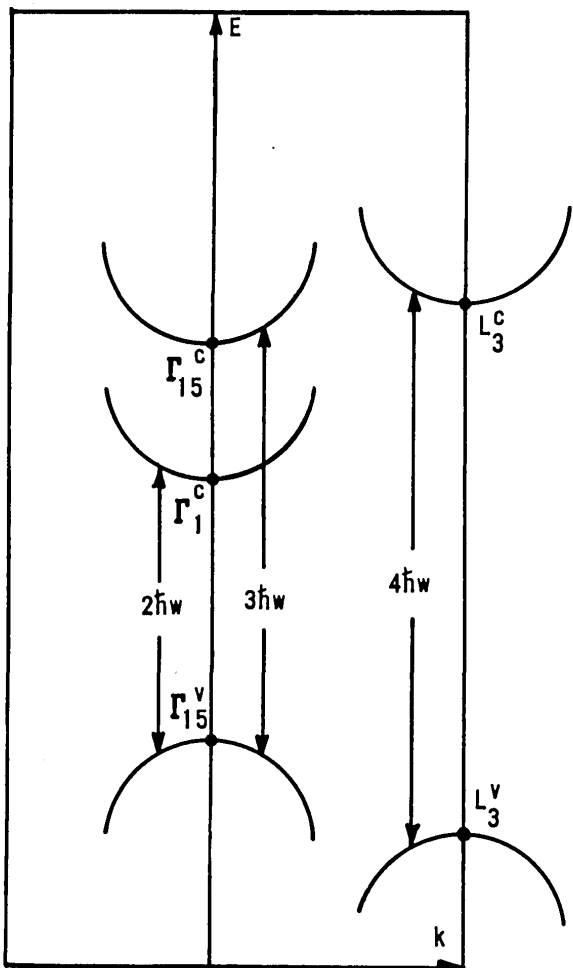


Fig. 9. Schematic of the band structure of GaP in the vicinity of Γ and L points (after Pyshkin *et al.*¹¹³).

sities ($>10^{26}$ photons/cm² sec), Δn increased with the fourth and fifth powers of I , characteristic of four and five-photon absorptions, respectively.

Pyshkin *et al.*¹¹³ explained this observation in terms of the band structure of GaP. They interpreted the two-, three-, and four-photon absorption as taking place in the neighborhood of the symmetry points Γ and L in the Brillouin zone of GaP, as shown in Fig. 9. They suggested that the oscillator strength for the transition between the states near L_3^v and L_3^c was substantially larger than the momentum matrix elements between Γ_{15}^v and Γ_{15}^c , which in turn was larger than the momentum matrix element connecting states close to Γ_{15}^v and Γ_1^c ; and this explained the observed variation of Δn with I . It is possible that the above experimental result can be explained from a different viewpoint. The theory of Keldysh³⁰ and Jones and Reiss³⁶ suggest that the effective energy gap of a crystalline solid in the presence of electromagnetic radiation increases with increasing radiation intensity and that at sufficiently high intensities it can be much larger than the ordinary field-free energy gap [see Eqs. (28) and (29)]. The physical significance of this increase in effective band-gap energy is that, with increasing radiation intensity, it takes more energy to oscillate the electrons in a given energy band and at the same time effect an interband transition (see Ref. 36). If this is true, a TPA process observed at low intensities may be energetically impossible at higher intensities because of the increased band gap, and a three-photon process may

be needed instead. At even higher intensities the effective direct-energy gap of GaP may be larger than the combined energies of three ruby photons, and a four-photon process is required, and so on. This field-induced effect, which may be considered an extension of the Franz-Keldysh effect to the case of alternating fields, may also be responsible for the experimentally observed variation of Δn with I (for further discussion and numerical results, see Ref. 114). Pyshkin *et al.* also noted a similar behavior with a Nd laser, for which at low intensities the generated carrier density varied as I^2 (at 129 and 172 K) because of a phonon-assisted two-photon transition from Γ to L points, or as I^3 (at 140 K) because of direct three-photon absorption at Γ point. However, at very high intensities ($>10^{27}$ photons cm⁻² sec), Δn was proportional to I^6 or I^7 because of direct transitions near L point. These observations indicate the importance of properly taking into account the temperature at which the MPA experiments are performed, especially in indirect-gap crystals, as well as the intensities used, which, if sufficiently high, might give rise to field-dependent effects such as the dynamic Franz-Keldysh effect.

5. RECOMMENDATIONS

In conclusion, we see that both theoretical and experimental research on multiphoton absorption processes have matured considerably since the pioneering work of Göppert-Mayer.⁴ In spite of an abundance of published work in both theoretical and experimental areas, there is still a disconcertingly large scatter among the results of different researchers. We have tried in this review to probe the origin of these large differences and gain a better understanding of the relative merits and deficiencies of different models and experimental techniques. Based on the material presented in this review, our main conclusions and recommendations are as follows.

The calculation and measurement of accurate and reliable MPA coefficients in crystalline solids is a nontrivial problem, even though it is conceptually simple. On the theoretical side, the results of simple analytical models are generally inaccurate and unreliable, because of their incompleteness by not fully taking into account all the parameters that influence the MPA coefficients. In order to obtain more-accurate and reliable results, use should be made of all pertinent solid-state data available, such as detailed band structures (electronic energy as functions of the magnitude and direction of the wave vector for different bands), accurate values of effective masses and momentum matrix elements, and band degeneracies. These calculations should include as many interband and intraband transitions as are needed to obtain good convergence in the final result. The role of excitons and impurities should also be taken into account. Field-induced phenomena, such as changes in the energy gap of the crystal and electronic wave functions, should be included for greater accuracy, especially at high intensities.

On the experimental side, the results are again easily affected by many parameters, such as sample size, orientation, impurity content, temperature, free-carrier absorption, degree of crystallinity, laser-pulse duration, spatial and temporal fluctuations, peak intensity, and polarization. Well-characterized crystalline samples and laser pulses are, therefore, a must for obtaining reliable results. It is recommended that future researchers list all the above experimental parameters

with the measured absorption coefficients in order to make comparisons with the results of other workers meaningful. In our consideration, whenever possible, high-sensitivity laser calorimetry and a two-channel normalization technique should be implemented.

ACKNOWLEDGMENT

V. Nathan was a U.S. Air Force Systems Command–National Research Council Postdoctoral Resident Research Associate when this research was started.

Vaidya Nathan was formerly A. Vaidyanathan.

Note added in proof: Recently M. A. Woodall et al. of North Texas State University, Denton, Texas 76203 (personal communication) measured the TPA coefficients of several semiconductors at 1.06 and 0.53 μm and found them to follow a $(1/n^2 E_g^3)$ dependence, where n is the refractive index and E_g is the minimum direct energy gap of the semiconductor.

REFERENCES

1. V. I. Bredikhin, M. D. Galanin, and V. N. Genkin, *Usp. Fiz. Nauk.* **110**, 3 (1973) [Sov. Phys. Usp. **16**, 299 (1973)].
2. H. Mahr, in *Quantum Electronics*, H. Rabin and C. L. Tang, eds. (Academic, New York, 1975), Vol. 1, Part A, p. 285.
3. J. M. Worlock, in *Laser Handbook*, F. T. Arecchi and E. O. Schulz-Dubois, eds. (North-Holland, Amsterdam, 1972), p. 1323.
4. M. Göppert-Mayer, *Ann. Phys. (Lieipzig)* **9**, 273 (1936).
5. R. Braunstein and N. Ockman, *Phys. Rev.* **134**, A499 (1964); see also R. Braunstein, *Phys. Rev.* **125**, 475 (1962).
6. C. C. Lee and H. Y. Fan, *Appl. Phys. Lett.* **20**, 18 (1972).
7. S. S. Mitra, L. M. Narducci, R. A. Shatas, Y. F. Tsay, and A. Vaidyanathan, *Appl. Opt.* **14**, 3038 (1975).
8. N. G. Basov, A. Z. Grasyuk, I. G. Zubarev, V. A. Katulin, and O. N. Kroklin, *Zh. Eksp. Teor. Fiz.* **50**, 551 (1966) [Sov. Phys. JETP **23**, 366 (1966)].
9. N. G. Basov, A. Z. Grasyuk, V. F. Efimkov, I. G. Zubarev, V. A. Katulin, and J. M. Popov, *J. Phys. Soc. Jpn. Suppl.* **21**, 277 (1966).
10. A. Vaidyanathan, T. Walker, A. H. Guenther, S. S. Mitra, and L. M. Narducci, *Phys. Rev. B* **20**, 3526 (1979).
11. R. Loudon, *Proc. Phys. Soc. London* **80**, 952 (1962).
12. G. D. Mahan, *Phys. Rev. Lett.* **20**, 332 (1968).
13. G. D. Mahan, *Phys. Rev.* **170**, 825 (1968).
14. A. I. Bobrysheva, S. A. Moskalenko, and M. I. Shmiglyuk, *Fiz. Tekh. Poluprov.* **1**, 1469 (1967) [Sov. Phys. Semicond. **1**, 1224 (1968)].
15. M. S. Bespalov, L. A. Kulevskii, V. P. Makarov, M. A. Prokhorov, and A. A. Tikhonov, *Zh. Eksp. Teor. Fiz.* **55**, 144 (1968) [Sov. Phys. JETP **28**, 77 (1969)].
16. A. R. Hassan, *Nuovo Cimento LXXB*, 21 (1970).
17. F. Bassani and A. R. Hassan, *Opt. Commun.* **1**, 371 (1970).
18. A. M. Danishevskii, E. A. Ivchenko, S. F. Kochegarov, and M. I. Stepanova, *Zh. Eksp. Teor. Fiz. Pis'ma Red.* **16**, 625 [Sov. Phys. JETP Lett. **16**, 440 (1972)].
19. E. L. Ivchenko and E. Yu. Perlin, *Fiz. Tverd. Tela* **15**, 2781 (1973) [Sov. Phys. Solid State **15**, 1850 (1974)].
20. S. B. Arifzhanov and E. L. Ivchenko, *Fiz. Tverd. Tela* **17**, 81 (1975) [Sov. Phys. Solid State **17**, 46 (1975)].
21. H. J. Fossum and D. B. Chang, *Phys. Rev. B* **8**, 2842 (1973).
22. E. O. Kane, *J. Phys. Chem. Solids* **1**, 249 (1957).
23. C. C. Lee and H. Y. Fan, *Phys. Rev. B* **9**, 3502 (1974).
24. C. R. Pidgeon, B. S. Wherrett, A. M. Johnston, J. Dempsey, and A. Miller, *Phys. Rev. Lett.* **42**, 1785 (1979).
25. A. Vaidyanathan, T. Walker, A. H. Guenther, S. S. Mitra, and L. M. Narducci, *Phys. Rev. B* **21**, 743 (1980).
26. A. Vaidyanathan, A. H. Guenther, and S. S. Mitra, *Phys. Rev. B* **22**, 6480 (1980).
27. G. W. Bryant, *Phys. Rev. B* **22**, 1992 (1980).
28. A. Vaidyanathan, A. H. Guenther, and S. S. Mitra, *Phys. Rev. B* **24**, 225 (1981).
29. M. L. Cohen and T. K. Bergstresser, *Phys. Rev.* **141**, 789 (1966).
30. L. V. Keldysh, *J. Eksp. Teor. Fiz.* **47**, 1945 (1964) [Sov. Phys. JETP **20**, 1307 (1965)].
31. W. V. Houston, *Phys. Rev.* **57**, 184 (1940).
32. M. H. Weiler, M. Reine, and B. Lax, *Phys. Rev.* **171**, 170 (1968).
33. Y. Yacoby, *Phys. Rev.* **169**, 610 (1968).
34. Y. A. Bychkov and A. M. Dykhne, *Zh. Eksp. Teor. Fiz.* **56**, 1734 (1970) [Sov. Phys. JETP **31**, 928 (1970)].
35. V. A. Kovarskii and E. Y. Perlin, *Phys. Status Solidi* **45**, 47 (1971).
36. H. D. Jones and H. R. Reiss, *Phys. Rev.* **16**, 2466 (1977).
37. L. M. Narducci, S. S. Mitra, R. A. Shatas, P. A. Pfeiffer, and A. Vaidyanathan, *Phys. Rev. B* **14**, 2508 (1976).
38. I. M. Catalano, A. Cingolani, and A. Minafra, *Phys. Rev. B* **9**, 707 (1974).
39. D. A. Kleinman, R. C. Miller, and W. A. Nordland, *Appl. Phys. Lett.* **23**, 243 (1973).
40. A. M. Danishevskii, A. A. Patrin, S. M. Ryvkin, and I. D. Yaroshetskii, *Zh. Eksp. Teor. Fiz.* **56**, 1457 (1969) [Sov. Phys. JETP **29**, 781 (1969)].
41. A. F. Gibson, C. B. Hatch, P. N. D. Maggs, D. R. Tilley, and A. C. Walker, *J. Phys. C* **9**, 3259 (1976).
42. E. M. Belenov and I. A. Poluektov, *Zh. Eksp. Teor. Fiz.* **64**, 446 (1969) [Sov. Phys. JETP **29**, 754 (1969)].
43. T. L. Gvardzhialadze, A. Z. Grasyuk, and V. A. Kovalenko, *Zh. Eksp. Teor. Fiz.* **64**, 446 (1973) [Sov. Phys. JETP **37**, 227 (1973)].
44. R. C. Miller and W. A. Nordland, *J. Appl. Phys.* **46**, 2177 (1975).
45. A. Miller, A. Johnston, J. Dempsey, J. Smith, C. R. Pidgeon, and G. D. Holah, *J. Phys. C* **12**, 4839 (1979).
46. R. L. Swofford and W. M. McClain, *Rev. Sci. Instrum.* **46**, 246 (1975).
47. J. P. Hermann and J. Ducuing, *Opt. Commun.* **6**, 101 (1972).
48. H. Lotem and R. T. Lynch, Jr., *Phys. Rev. Lett.* **37**, 334 (1976).
49. H. Lotem and C. B. de Araujo, *Phys. Rev. B* **16**, 1711 (1977).
50. M. Bass, E. W. Van Stryland, and A. F. Stewart, *Appl. Phys. Lett.* **34**, 142 (1979).
51. B. M. Ashkinadze, S. L. Pyshkin, S. M. Ryvkin, and I. D. Yaroshetskii, *Fiz. Tekh. Poluprov.* **1**, 1017 (1967) [Sov. Phys. Semicond. **1**, 850 (1968)].
52. B. V. Zubov, L. A. Kulevskii, V. P. Makarov, T. M. Murina, and A. M. Prokhorov, *Zh. Eksp. Teor. Fiz. Pis'ma Red.* **9**, 221 (1969) [Sov. Phys. JETP Lett. **9**, 130 (1969)].
53. J. M. Ralston and R. K. Chang, *Appl. Phys. Lett.* **15**, 164 (1969).
54. J. M. Ralston and R. K. Chang, *Opto-Electron.* **1**, 182 (1969).
55. I. M. Catalano, A. Cingolani, and A. Minafra, *Phys. Rev. B* **5**, 1629 (1972).
56. I. M. Catalano, A. Cingolani, and A. Minafra, *Opt. Commun.* **5**, 212 (1972).
57. D. Frohlich and B. Staginnus, *Phys. Rev. Lett.* **19**, 496 (1967).
58. R. G. Wenzel, G. P. Arnold, and N. R. Greiner, *Appl. Opt.* **12**, 2245 (1973).
59. I. M. Catalano, A. Cingolani, and A. Minafra, *Solid State Commun.* **16**, 417 (1975).
60. S. J. Bepko, *Phys. Rev. B* **12**, 669 (1975).
61. A. Z. Grasyuk, I. G. Zubarev, A. B. Mironov, and I. A. Poluektov, *Kvantovaya Elektron. (Moscow)* **2**, 1826 (1975) [Sov. J. Quantum Electron. **5**, 997 (1976)].
62. A. Z. Grasyuk, I. G. Zubarev, A. B. Mironov, and I. A. Poluektov, *Fiz. Tekh. Poluprov.* **10**, 262 (1976) [Sov. Phys. Semicond. **10**, 159 (1976)].
63. A. Penzkofer and W. Falkenstein, *Opt. Commun.* **17**, 1 (1976).
64. A. Penzkofer and W. Falkenstein, *Opt. Commun.* **16**, 247 (1976).
65. I. G. Zubarev, A. B. Mironov, and S. I. Mikhailov, *Fiz. Tekh. Poluprov.* **11**, 415 (1977) [Sov. Phys. Semicond. **11**, 239 (1977)].

66. F. Adduci, I. M. Catalano, A. Cingolani, and A. Minafra, Phys. Rev. B 15, 926 (1977).
67. J. F. Reintjes and R. Eckardt, IEEE J. Quantum Electron. QE-13, 791 (1977).
68. B. Bosacchi, J. S. Bessey, and F. C. Jain, J. Appl. Phys. 49, 4609 (1978).
69. J. Dempsey, J. Smith, G. D. Holah, and A. Miller, Opt. Commun. 26, 265 (1978).
70. P. Liu, W. L. Smith, H. Lotem, J. H. Bechtel, N. Bloembergen, and R. S. Adhhav, Phys. Rev. B 17, 4620 (1978).
71. P. Liu, R. Yen, and N. Bloembergen, Appl. Opt. 18, 1015 (1979).
72. A. F. Stewart and M. Bass, Appl. Phys. Lett. 37, 1040 (1980).
73. I. M. Catalano and A. Cingolani, Phys. Rev. B 19, 1049 (1979).
74. I. M. Catalano and A. Cingolani, J. Appl. Phys. 50, 5638 (1979).
75. A. M. Johnston, C. R. Pidgeon, and J. Dempsey, Phys. Rev. B 22, 825 (1980).
76. A. Miller and G. S. Ash, Opt. Commun. 33, 297 (1980).
77. A. A. Borshch, M. S. Brodin, and N. N. Krupa, Zh. Eksp. Teor. Fiz. 70, 1805 (1975) [Sov. Phys. JETP 43, 940 (1976)].
78. I. M. Catalano and A. Cingolani, Solid State Commun. 34, 761 (1980).
79. J. P. Van der Ziel, Phys. Rev. B 16, 2775 (1977).
80. M. Casalboni, F. Crisanti, R. Francini, and U. M. Grassano, Solid State Commun. 35, 833 (1980).
81. A. Cingolani, F. Ferrero, A. Minafra, and D. Trigiante, Nuovo Cimento 4B, 217 (1971).
82. J. H. Bechtel and W. L. Smith, Phys. Rev. B 13, 3515 (1976).
83. Y. A. Oksman, A. A. Semenov, V. N. Smirnov, and O. M. Smirnov, Fiz. Tekh. Poluprov. 6, 731 (1972) [Sov. Phys. Semicond. 6, 629 (1972)].
84. A. Z. Grasyuk, I. G. Zubarev, V. V. Lobko, Y. A. Matveets, A. B. Mironov, and O. B. Shatherashvili, Zh. Eksp. Teor. Fiz. Pis'ma Red. 17, 584 (1973) [Sov. Phys. JETP Lett. 17, 416 (1973)].
85. V. V. Arsenev, V. S. Dneprovskii, D. N. Klyshko, and A. N. Penin, Zh. Eksp. Teor. Fiz. 56, 760 (1969) [Sov. Phys. JETP 29, 413 (1969)].
86. S. Jayaraman and C. H. Lee, J. Appl. Phys. 44, 5480 (1973).
87. I. M. Catalano, A. Cingolani, and A. Minafra, Opt. Commun. 11, 254 (1974).
88. H. J. Fossum and D. B. Chang, Phys. Rev. B 8, 2842 (1973).
89. J. M. Doviak, A. F. Gibson, M. F. Kimmitt, and A. C. Walker, J. Phys. C 6, 593 (1973).
90. B. M. Ashkinadze, A. I. Bobrysheva, E. V. Vitiu, V. A. Kovarskii, A. V. Lelyakov, S. A. Moscalenko, S. L. Pyshkin, and S. I. Radautsan, in *Proceedings of the Ninth International Conference on the Physics of Semiconductors* (Nauk, Moscow, 1968), p. 189.
91. V. A. Kovarskii and E. V. Vitiu, Fiz. Tek. Poluprov. 3, 421 (1969) [Sov. Phys. Semicond. 3, 354 (1969)].
92. J. H. Yee, J. Phys. Chem. Solids 33, 643 (1972).
93. J. H. Yee and H. H. M. Chau, Opt. Commun. 10, 56 (1974).
94. J. H. Yee, Phys. Rev. B 5, 449 (1972).
95. F. Bassani and A. R. Hassan, Nuovo Cimento 7B, 313 (1972).
96. F. Herman, R. L. Kortum, C. D. Kuglin, and R. A. Short, J. Phys. Soc. Jpn. Suppl. 21, 7 (1966).
97. F. H. Pollak, C. W. Higginbotham, and M. Cardona, J. Phys. Soc. Jpn. Suppl. 21, 20 (1966).
98. A. R. Hassan, Nuovo Cimento 13B, 19 (1973).
99. J. F. Reintjes and J. C. McGroddy, Phys. Rev. Lett. 30, 901 (1973).
100. A. I. Bobrysheva and S. A. Moskalenko, Fiz. Tekh. Poluprov. 3, 1601 (1969) [Sov. Phys. Semicond. 3, 1347 (1970)].
101. S. S. Mitra, N. H. K. Judell, A. Vaidyanathan, and A. H. Guenther, Opt. Lett. 7, 307 (1982).
102. B. M. Ashkinadze and I. D. Yaroshetskii, Fiz. Tekh. Poluprov. 1, 1706 (1967) [Sov. Phys. Semicond. 1, 1413 (1968)].
103. V. V. Arsenev, V. S. Dneprovskii, D. N. Klyshko, and L. A. Sysoev, Zh. Eksp. Teor. Fiz. 60, 114 (1971) [Sov. Phys. JETP 33, 64 (1971)].
104. B. M. Ashkinadze, S. M. Ryvkin, and I. D. Yaroshetskii, Fiz. Tekh. Poluprov. 2, 1540 (1968) [Sov. Phys. Semicond. 2, 1285 (1969)].
105. V. S. Dneprovskii, D. N. Klyshko, and A. N. Penin, Zh. Eksp. Teor. Fiz. Pis'ma Red. 10, 385 (1966) [Sov. Phys. JETP Lett. 3, 251 (1966)].
106. G. I. Aseev, M. L. Kats, and V. K. Nikol'skii, Zh. Eksp. Teor. Fiz. Pis'ma Red. 8, 174 (1968) [Sov. Phys. JETP Lett. 8, 103 (1968)].
107. B. M. Ashkinadze, I. P. Kretsu, S. L. Psyhkin, and I. D. Yaroshetskii, Fiz. Tek. Poluprov. 2, 1511 (1968) [Sov. Phys. Semicond. 2, 1261 (1969)].
108. E. L. Ivchenko and E. Yu. Perlin, Fiz. Tverd. Tela. 15, 2781 (1973) [Sov. Phys. Solid State 15, 1850 (1974)].
109. A. M. Danishevskii, S. F. Kochegarov, and V. K. Subashiev, Zh. Eksp. Teor. Fiz. 70, 158 (1976) [Sov. Phys. JETP 43, 83 (1976)].
110. S. B. Arifzhanov, A. M. Danishevskii, E. L. Ivchenko, S. F. Kochegarov, and V. K. Subashiev, Zh. Eksp. Teor. Fiz. 74, 172 (1978) [Sov. Phys. JETP 47, 88 (1978)].
111. A. R. Hassan and R. Raouf, Phys. Status Solidi B104, 703 (1981).
112. J. H. Yee, Phys. Rev. B 3, 355 (1971).
113. S. L. Pyshkin, N. A. Ferdman, S. I. Radutsan, V. A. Kovarsky, and E. V. Vitiu, Opto-Electron. 2, 245 (1970).
114. A. Vaidyanathan and A. H. Guenther, Phys. Status Solidi B 112, K73 (1982).